Review | Received 26 November 2025; Revised 15 December 2025; Accepted 16 December 2025; Published 29 December 2025
https://doi.org/10.55092/aimat20250017

Physics-informed artificial intelligence for solid oxide cells: a comprehensive review of frameworks, applications, and prospects for digital twins

Yibin Zhang[1,2], Min Zhang[1,2], Chengzhi Guan[1,2,3,*], Fei Deng[4], Shixue Liu[4,*], Zijing Lin[5] and Jianqiang Wang[1,2,3]

[1] Shanghai Institute of Applied Physics, Chinese Academy of Sciences, Shanghai, China
[2] University of Chinese Academy of Sciences, Beijing, China
[3] Shanghai Hyenergy Technology Co., Ltd., Shanghai, China
[4] Hydrogen Energy Industrial Technology Innovation Center, China Nuclear Power Technology Research Institute, Shenzhen, China
[5] Department of Physics, University of Science and Technology of China, Hefei, China

* Correspondence authors; E-mails: guanchengzhi@sinap.ac.cn (C.G.); liushixue@cgnpc.com.cn (S.L.).

Highlight:

- Proposes a hierarchical PIAI framework for SOCs comprising three paradigms: loss-level injection, architecture-level fusion, and integration-level correction.
- Demonstrates how PIAI enables multiscale coupling (microstructure to stack-level) and supports Digital Twin deployment.
- Identifies key methodological challenges, including spectral bias, multi-fidelity data fusion, and uncertainty quantification, and discusses strategies for robust, scalable solid oxide cells twins.
- Bridges cross-domain advances in physics-informed artificial intelligence framework from other electrochemical systems (e.g., proton exchange membrane cells, Li-ion batteries) to the solid oxide cells field, highlighting transferable architectures and emerging research frontiers.

Abstract: Solid oxide cells (SOCs) are a cornerstone technology for sustainable energy conversion, enabling efficient, bidirectional transformation between electrical and chemical energy. However, large-scale deployment is constrained by complex, multi-scale electrochemical-thermal-mechanical processes, rendering accurate modeling and real-time control computationally prohibitive. Traditional physics-based models (e.g., CFD, FEA) offer high-fidelity but are costly and inflexible, whereas purely data-driven models lack physical interpretability and generalization under out-of-distribution conditions. To bridge this gap, the emerging paradigm of physics-informed artificial intelligence integrates physical laws, governing equations, and mechanistic knowledge into machine learning frameworks, thereby achieving a balance between physical consistency, computational efficiency, and data adaptability. This review provides a systematic synthesis of physics-informed artificial intelligence methodologies in the solid oxide cells domain and introduces a hierarchical taxonomy encompassing three progressively

integrated paradigms: loss-level physics injection, architecture-level fusion, and integration-level correction. These paradigms reflect an evolution from externally constrained learning to fully coupled hybrid intelligence, aligning with the increasing complexity of solid oxide cells modeling and digital twins deployment. Representative applications across microstructural evolution, stack-level performance mapping, degradation diagnosis, and optimization are analyzed to illustrate how physics-informed artificial intelligence enhances interpretability, robustness, and scalability in practical solid oxide cells workflows. Finally, the review identifies key challenges—such as spectral bias, multi-fidelity data fusion, and uncertainty quantification—and highlights emerging directions including neural operators, Bayesian deep learning, and hybrid digital twins architectures to accelerate the physics-artificial intelligence convergence toward reliable, real-time, and lifecycle-aware solid oxide cells engineering.

Keywords: solid oxide cells; physics-informed machine learning; digital twins; multi-physics modeling; model predictive control

1. Introduction

Amid global decarbonization efforts and the transformation of energy systems, the importance of efficient and flexible energy conversion and storage technologies is increasingly recognized. SOCs are high- temperature electrochemical devices capable of bidirectional operation in both fuel cell (SOFC) and electrolysis (SOEC) modes, offering diverse fuel options and high system-level efficiency. They are emerging as a key technology to support the integration of renewable and hydrogen energy systems [1]. Recent reviews and assessment reports have comprehensively outlined the advantages, application scenarios, and technological advancements of SOCs, offering strong support for the engineering strategy of high-efficiency coupling and large-scale demonstration [2,3].

Meanwhile, the engineering deployment of SOCs is limited by the modeling and control complexity induced by cross-scale structures and multi-physics coupling. Sole reliance on experiments is costly and time-consuming. Traditional high-fidelity white-box models (e.g., CFD/FEA) provide detailed analyses but are computationally intensive and cannot support real-time monitoring or online optimization. By contrast, purely data-driven black-box models are vulnerable to instability under sparse data and out-of-distribution (OoD) conditions, and they often lack physical consistency and interpretability, thereby diminishing the credibility and transferability of engineering decisions. These observations have been repeatedly corroborated by reviews on SOFC modeling and durability, as well as by benchmark studies of data-driven methods [4,5].

In this context, the digital twins (DTs) are regarded as a key paradigm that bridges physical fidelity and engineering real-time operation. It leverages a dynamically consistent virtual replica of the physical system to integrate microstructural evolution, state estimation, and system-level optimal control.

The DTs for SOCs are defined as a bidirectionally coupled virtual replica of the physical system, enabling synchronization between simulation, sensing, and control. Physics-informed artificial intelligence (PIAI) enhances DTs by embedding physics-consistent surrogates within the twins loop:

- Data assimilation layer: integrates sensor and operational data through Bayesian or operator-learning surrogates;
- Modeling layer: employs PIAI surrogates (e.g., Physics-Informed Neural Networks (PINN), Fourier Neural Operators (FNO), and Deep Operator Networks (DeepONet)) for fast field reconstruction;

- Decision layer: connects to model predictive control (MPC) for lifetime-aware optimization and fault diagnosis.

Key performance indicators (KPIs) include latency, physical-consistency score, and generalization robustness.

However, realizing a highly reliable and deployable SOCs DTs requires a new balance between physical fidelity and computational cost [6,7]. PIAI improves physical consistency, generalization, and inference efficiency under small-sample and noisy conditions by explicitly embedding conservation laws and governing equations (often expressed as PDEs) during training, thereby providing a powerful approach for real-time prediction, online optimization, and lifecycle management of SOCs [8–10].

Unlike existing reviews [11,12] that primarily survey general AI applications or focus on specific fuel cell types, this work establishes a comprehensive three-tier PIAI framework: Loss-level, Architecture-level, and Integration-level, specifically tailored for the multi-scale coupling challenges of SOCs. This hierarchical taxonomy provides a structured pathway for engineers to select appropriate AI interventions based on their specific modeling fidelity and data availability requirements. Table 1 summarizes the latest typical applications of ML in the SOCs field.

Table 1. Latest typical applications of ML in the SOCs field.

Task	Key Metrics	Best Results
SOFC ML Design Optimization [13]	Optimize SOFC geometry and flow rates to minimize Temperature Gradient and Cost per Watt and maximize Power Density	Gaussian Process Regression (GPR) achieved best performance, with nRMSE for power density at 0.0052 W/cm^2; Max power density reached 2.45 W/cm^2; Minimum temperature gradient achieved was 7.7 °C.
Real-Time SOEC Model [14]	Real-time execution capability; Maximum Relative Error; Transient Local Solid Temperature Gradient	Real-Time Execution: Achieved at 5 ms fixed time step (up to 640 nodes); Critical Risk: Peak temperature gradient magnitude nearly doubled in 10 s during transients.
SOFC Parameter Estimation [15]	Estimate six critical SOFC parameter under varying pressure (1–5 atm).	Accuracy: Minimum Mean Squared Error (MSE) as low as 0.52 (at 5 atm). Efficiency: Converged in 3.7 s (40%–60% faster than competing algorithms). Robustness: Predictive deviation ≤ 5% from experimental data.
SOEC ML Performance Prediction [16]	Predict cell voltage and polarization curves of LSM-YSZ/YSZ/Ni-YSZ cells using ML models (XGBoost, RF, ANN, SVR).	Best Model: Extreme Gradient Boosting (XGBoost) was superior. Accuracy: 98.39% for cell voltage prediction and 98.10% for IV curve interpolation.

The structure of this paper is organized as follows: Section 2 outlines the fundamental modeling challenges in SOCs. Section 3 details the proposed three-tier PIAI framework. Section 4 analyzes representative applications across different scales. Section 5 discusses key implementation challenges, and Section 6 provides an outlook on future digital twin developments.

2. Solid oxide cells: fundamentals and the modeling imperative

2.1. Technology overview and operating principles

SOCs are electrochemical devices that operate at medium to high temperatures (typically 600–1000 °C) and employ electrolytes that conduct oxygen ions (O-SOCs) or protons (H-SOCs). They support bidirectional operation—SOFC (chemical→electrical) and SOEC (electrical→chemical)—and can operate reversibly within the same stack (reversible SOCs, rSOCs) [17]. In SOFC mode, fuel is oxidized

at the anode, releasing electrons to an external circuit, while oxidant (e.g., air) is reduced at the cathode. In SOEC mode, the process is reversed; electrical energy drives the reduction of steam at the cathode (in H-SOCs) or anode (in O-SOCs) to produce hydrogen [18]. Figure 1 illustrates the internal reactions of O/H-rSOCs operating in both FC and EC modes. The elevated operating temperature accelerates electrode kinetics and enables high-grade waste-heat recovery, thereby accommodating diverse fuels (e.g., H_2, CO/syngas, reformed natural gas, ammonia) and delivering higher system-level efficiency. SOCs are well suited for integration with waste-heat recovery, cogeneration of power and hydrogen, and renewable-energy utilization [19,20].

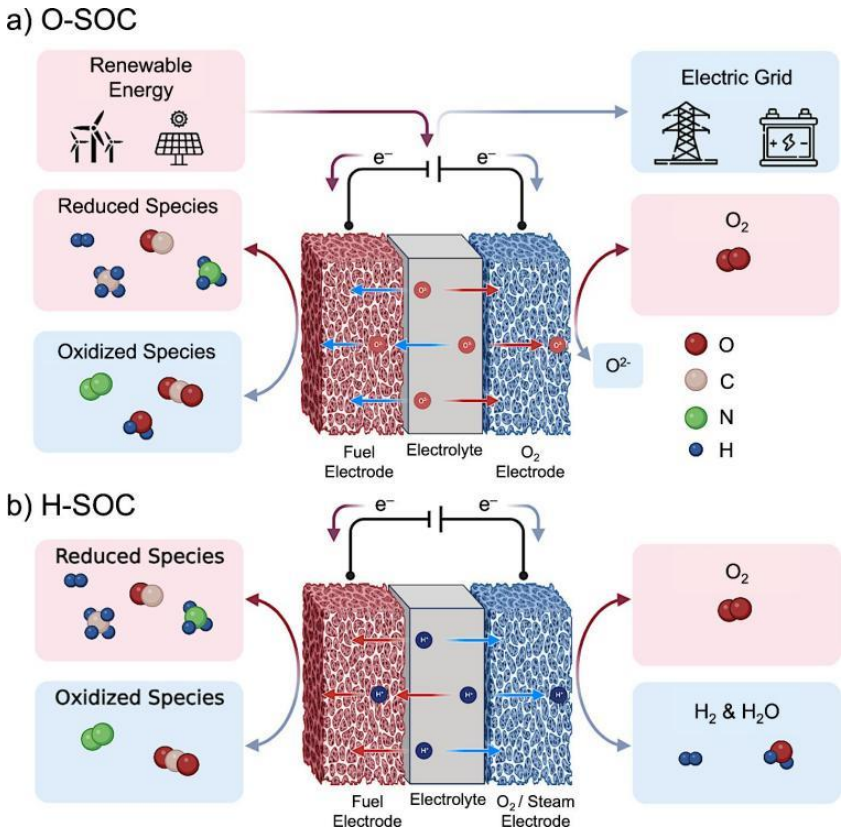

Figure 1. Schematic of a reversible **(a)** O-SOC and **(b)** H-SOC. Red arrows represent the pathway for the electrolysis mode. Blue arrows represent the pathway for the fuel cell mode [19]. Reprinted with permission. Copyright 2024 Chemical Reviews.

The typical electrode and overall reaction equations for hydrogen-fueled, O-SOCs in both operating modes (SOFC and SOEC) are as follows:

(1) Fuel Cell Mode (SOFC)

Cathode (air side):

$$\frac{1}{2}O_2 + 2e^- \rightarrow O^{2-}$$

Anode (fuel side):

$$H_2 + O^{2-} \rightarrow H_2O + 2e^-$$

Overall reaction:

$$H_2 + \frac{1}{2}O_2 \rightarrow H_2O$$

(2) Electrolysis Mode (SOEC, Steam Electrolysis)

Cathode (fuel side):

$$H_2O + 2e^- \rightarrow H_2 + O^{2-}$$

Anode (air side):

$$O^{2-} \rightarrow \frac{1}{2}O_2 + 2e^-$$

Overall reaction:

$$H_2O \rightarrow H_2 + \frac{1}{2}O_2$$

The high operating temperature is a double-edged sword. It obviates the need for expensive noble metal catalysts and enables high reaction rates and system efficiencies. However, it also accelerates degradation mechanisms and imposes severe material compatibility and thermal management challenges [21].

2.2. Key challenges and degradation mechanisms

Alongside these advantages, several key challenges persist: chemical compatibility and phase stability at electrode-electrolyte interfaces; redox-cycling—induced embrittlement, carbon deposition, and sulfur poisoning of Ni-based anodes; chromium volatilization from interconnects and CO_2-induced carbonation at the cathode; and microstructural degradation driven by thermal stresses and thermal cycling [18,22]. These issues have been systematically reviewed in the materials and durability literature, and recent studies on sulfur/halogen contamination, chromium poisoning/deposition mechanisms, and thermal-management strategies have clarified the mechanisms and advanced corresponding mitigation measures [5,21,23].

Specifically, the chemical compatibility and phase stability at the cathode-electrolyte interface are decisive for both early-stage performance and long-term durability: in lanthanum strontium cobalt ferrite/yttria-stabilized zirconia (LSCF/YSZ) stacks, insulating $La_2Zr_2O_7$ and $SrZrO_3$ phases readily form during sintering and operation, thereby increasing interfacial resistance and depleting active sites [24,25]. To mitigate such parasitic reactions, engineers commonly insert ceria-based diffusion barriers—Gd-doped ceria (GDC) or Sm-doped ceria (SDC)—yet interdiffusion and densification at the barrier/substrate and barrier/electrode interfaces can add extra series resistance; consequently, barrier thickness and thermal-treatment parameters must be carefully optimized [26,27].

On the fuel side, Ni-based anodes exposed to hydrocarbons or syngas readily undergo surface catalytic cracking and the Boudouard reaction, which trigger carbon deposition, shortening of the triple-phase boundary (TPB) length, and pore blockage. Figure 2 illustrates the carbon deposition behavior and corresponding morpgical evolution of Ni/YSZ composite electrodes after exposure to humidified methane at different temperatures. Targeted countermeasures include increasing the steam partial pressure, optimizing the anode microstructure, and deploying alloy and oxide promoters [28,29]. Sulfur impurities (e.g., H_2S) form adsorbed/sulfidized layers on Ni that suppress electrochemical kinetics; the poisoning is partially reversible at low overpotential but becomes increasingly irreversible under high overpotential and prolonged loading. Accordingly, materials modifications and operational strategies—raising temperature, increasing steam content, and applying short oxidation-reduction cleaning cycles—can enhance tolerance and partially restore activity [22,30]. During operating transients or fuel interruption, Ni-NiO redox cycling induces substantial volume changes and pore collapse, causing

cracking, interlayer delamination, and a reduction in TPB density; this constitutes an independent degradation pathway that synergistically amplifies the aforementioned chemical poisoning. The damage threshold and accumulation rate are governed primarily by temperature, steam content/humidity, and cycling frequency, thereby providing quantitative targets for microstructural design and alloying [31–33].

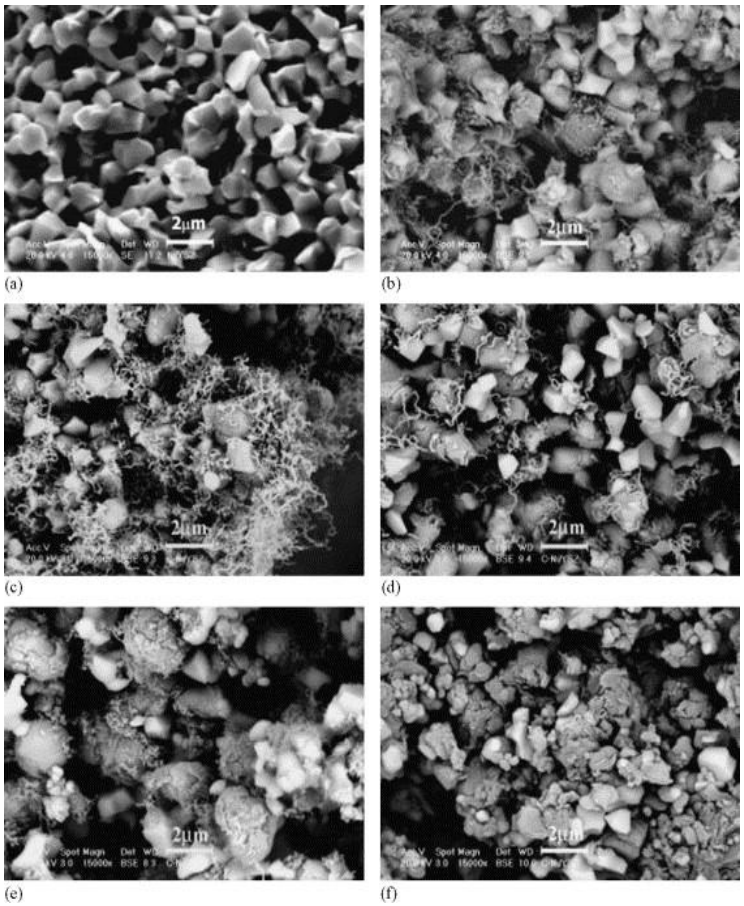

Figure 2. SEM images of Ni/YSZ **(a)** as-prepared, and after carbon deposition in humidified methane for 4 h at **(b)** 500 °C, **(c)** 600 °C surface, **(d)** 600 °C, **(e)** 700 °C, and **(f)** 800 °C. All images are from the center of the pellet except for **(c)** [34]. Reprinted with permission. Copyright 2007 Applied Catalysis A: General.

On the air side, ferritic stainless-steel (FSS) interconnects generate volatile chromium species in humid oxygen atmospheres; these species deposit on the cathode and react with surface Sr to form inert phases, thereby raising the polarization resistance. Spinel coatings such as Mn-Co oxide can markedly suppress chromium evaporation and deposition, reducing evaporation rates by 50- to 100- fold over 500 h of exposure [23,35,36]. Concurrently, in atmospheres containing CO_2 and water vapor, Sr-enriched surface layers are more prone to carbonate formation, leading to a decrease in the surface exchange coefficient and an increase in interfacial resistance; CO_2 further accelerates outward Sr migration toward a quasi-steady state [37,38]. Further studies indicate that under oxygen-rich or CO_2-rich conditions, carbonate formation is thermodynamically more favorable; the associated processes exhibit strong dependences on temperature and partial pressures and can be mitigated via surface overlayers and the design of CO_2-tolerant cathode materials [39,40]. Beyond these exogenous species, trace halogens (e.g., HCl) can rapidly diminish anode activity and induce irreversible degradation, with more pronounced effects under current load, underscoring

the need for stringent control of fuel-gas purity and cleanup protocols [41]. Figure 3 illustrates that under electrolysis operation with applied current load, even trace amounts of HCl markedly increase the anode charge-transfer resistance and induce irreversible performance degradation, indicating that chlorine poisoning becomes more severe under polarization conditions.

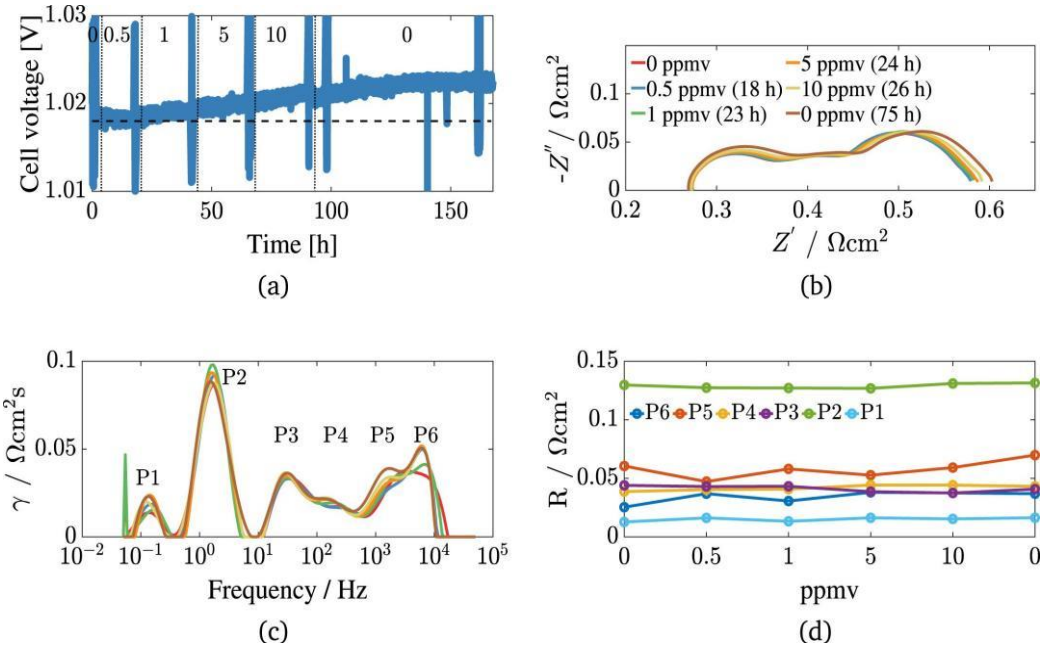

Figure 3. Effect of HCl concentration on SOEC performance and impedance under polarization [41]. Reprinted with permission. Copyright 2021 Journal of Power Sources.

These chemical and electrochemical degradation processes ultimately couple with thermos-mechanical phenomena at the stack-level and are amplified by temperature gradients and thermal cycling: micro-cracking, delamination, and seal failure are common outcomes, and both open-circuit voltage (OCV) and output power exhibit measurable declines with repeated cycles. Consequently, engineering-oriented burner/heat-exchanger design, flow-rate and recirculation-ratio scheduling, and thermal-subsystem modeling and control have been shown to reduce peak ΔT, alleviate thermal stresses, and improve reliability [42,43]. Taken together, chromium deposition and CO_2-H_2O atmospheres synergistically accelerate cathode deactivation, whereas anode coking and sulfur films raise local overpotentials and exothermicity, thereby increasing thermal stresses and Ni-NiO redox risk. It follows that only coordinated optimization across the materials, interface, operational, and system levels can achieve a robust balance between lifetime and efficiency [23,44].

2.3. The modeling bottleneck in SOCs engineering

The development and deployment of SOCs are critically dependent on computational models, yet engineering practice still encounters four recurrent challenges: (i) large model uncertainty induced by strongly coupled multi-physics, cross-scale degradation, and the prohibitive cost of high-fidelity simulations [2,45,46]; reconstruction and extrapolation of in-stack temperature, species concentration, and current-density fields under sparse sensing [47–49]; (ii) online identification of kinetic and heat/mass-transfer parameters under time-varying operation and aging [50,51]; and (iii) system-level optimization and real-time control subject to tight thermal-mass-electrical constraints [52,53].

From a methodological perspective, SOC modeling today is polarized between two extremes. High-fidelity white-box models that resolve coupled charge, mass, momentum, and heat transport with detailed electrochemistry offer predictive accuracy but are computationally expensive at stack and system levels, making them impractical for uncertainty propagation, large-scale optimization, or embedded control [2,43,45]. In contrast, purely data-driven black-box models (e.g., generic neural networks or Gaussian processes trained solely on data) deliver millisecond-level inference but may violate conservation principles, extrapolate poorly outside the training domain, and provide limited interpretability and decision-grade uncertainty quantification (UQ)—issues repeatedly emphasized in the explainable AI (XAI) and ML methodology literature [54,55].

Bridging this dichotomy motivates a hybrid, physics-integrated paradigm in which data-driven surrogates, data assimilation, and state estimation are constrained by governing laws and priors, thereby improving extrapolation, trustworthiness, and deployability. Recent surveys of physics-informed machine learning (PIML) document how embedding conservation laws, constitutive relations, and structural priors into learning pipelines enhances generalization and stabilizes predictions for energy and thermo-fluid systems, suggesting a natural fit for SOC stacks and balance-of-plant [56–58].

Practically, this implies: using high-fidelity models judiciously to generate targeted design of experiments and supervisory priors; training reduced-order or operator-learning surrogates on those priors while enforcing thermodynamic and transport constraints; applying observer/estimator schemes to fuse sparse measurements with model states in real-time; and closing the loop with MPC/nonlinear MPC that explicitly constrains ΔT, thermal stress, and fuel/air utilization. Such workflows directly address items (i)–(iii) above while satisfying safety and controllability requirements in deployment [59,60].

3. PIAI framework

Building on the preceding motivations, this paper introduces PIAI as a unified paradigm to balance physical fidelity, computational affordability, and data accessibility. The core idea is to embed conservation laws, governing equations, and boundary/initial conditions into the learning process to explicitly constrain model behavior. The learning objective is jointly optimized with limited experimental and high-fidelity simulation data, enabling physical consistency, robust generalization, and low-latency inference even under data-scarce and OoD conditions.

3.1. Foundational concepts of PIAI

Within PIAI paradigm discussed here, the widely used PINN unifies first-principles physics knowledge with data-misfit terms from sensors or high-fidelity simulations in a single optimization objective. The basic approach constructs PDEs residuals via automatic differentiation at spatiotemporal collocation points and jointly minimizes them with observation errors, thereby producing solutions that respect physical constraints even when data are scarce or unlabeled. A minimal loss function can be written as:

$$L = \lambda_{PDE}\,\mathrm{MSE}\;\; N\;[u_\theta]\;\; + \lambda_{BC/IC}\,\mathrm{MSE}\;\; B\;[u_\theta] - g\;\; + \lambda_{data}\,\mathrm{MSE}\;\; u_\theta - y' \tag{1}$$

This composite loss simultaneously enforces physical laws and data consistency, serving as the mathematical backbone of PINN-based PIAI. In this objective, $\boldsymbol{N}\,[\cdot]$ denotes the governing differential operator, used to compute residuals via automatic differentiation at collocation points; $\boldsymbol{B}\,[\cdot] = g$ represents

the initial/boundary conditions (IC/BC); u_θ is the network-predicted field; y denotes measured or high-fidelity data; and MSE $(\cdot)$ is the mean-squared error evaluated on the corresponding point sets.

In this objective, the weights λ_{PDE}, $\lambda_{BC/IC}$ and λ_{data} balance the trade-off between physical consistency and data fidelity. In practice, these weights are often dynamically adjusted; for instance, algorithms like GradNorm or relative loss balancing are used to prevent the data loss from dominating the small PDE residuals. A typical starting configuration might be $\lambda_{data} = 1$ and $\lambda_{PDE} = 0.1$, which is then adaptively updated during training to ensure convergence.

It is worth noting that, although a variety of AI algorithms incorporating physical priors have emerged in recent years, their applications in SOCs remain scarce. Nevertheless, several successful demonstrations in other complex engineered systems have verified the feasibility and promise of such paradigms. For instance, Kazuma *et al.* recently applied the DeepONet framework to DTs-based online monitoring of nuclear systems, illustrating how physics-informed operators can enable real-time prediction and anomaly detection in highly coupled multi-physics environments [61]. This example illustrates that the underlying concept of physics-informed learning extends beyond PINN, providing evidence for its scalability to complex coupled systems. These advances substantiate the potential of PIAI approaches for complex engineered systems. Nevertheless, because PINN remains the most extensively implemented form of physics-informed learning in SOCs, this review centers its foundational discussion on the PINN methodology, while the three subsequent frameworks—loss-level injection, architecture-level fusion, and integration-level correction—generalize this concept beyond PINN-specific formulations, emphasizing physical priors as the invariant core.

3.2. A taxonomy of PIAI intervention pathways

PIAI can be broadly defined as a hybrid learning paradigm that infuses physical laws, governing equations, or mechanistic priors into data-driven models to ensure physical consistency, enhance generalization, and enable real-time decision-making under data scarcity. Unlike purely empirical machine learning, which infers correlations directly from data, PIAI explicitly embeds physics either as loss constraints, structural priors, or multi-model couplings, allowing the network to learn not only from data but also from the underlying conservation and constitutive principles. Within the SOCs domain, PIAI serves as a bridge between high-fidelity simulation and operational intelligence, linking first-principles modeling with DTs deployment for performance prediction, degradation diagnosis, and control-oriented optimization.

Building on this foundation, the taxonomy proposed here delineates how physical knowledge intervenes across different layers of learning. Although PINN is the most recognizable form of PIAI, the broader landscape extends far beyond it. Current implementations differ mainly in how and where physics intervenes in the learning pipeline. To establish a coherent synthesis, this review adopts a hierarchical taxonomy of three paradigms: loss-level injection, architecture-level fusion, and integration-level correction. These correspond respectively to enforcing physics as an external constraint, embedding it as an internal structure, and orchestrating it as a cross-model interaction (Figure 4). This sequence delineates an evolutionary pathway from constraint→structure→interaction, reflecting a progressive deepening of physical coupling and engineering maturity in SOCs research.

(1) Loss-level physics injection (Figure 4a). Physics acts as an external constraint during optimization. PDE residuals, boundary/initial conditions (IC/BC), and data-misfit terms are jointly minimized to enforce conservation and continuity under sparse data. This pathway underlies field

reconstruction, parameter inversion, and feasibility mapping tasks in SOCs, where physical consistency outweighs data abundance.

(2) Architecture-level fusion (Figure 4b). Here, physics becomes part of the model's structure. Mechanistic priors—analytical surrogates, reduced-order outputs, or conservation features—are embedded as network branches or feature channels, transforming physics from a soft regularization signal into a hard structural prior. This enhances interpretability and sample efficiency, supporting microstructure-performance mapping and physics-aware diagnostics for SOCs electrodes.

(3) Integration-level correction (Figure 4c). At this level, physics regulates the interaction among models. Mechanistic solvers or reduced-order models (ROM) act as interpretable backbones, while AI surrogates serve as residual correctors or dynamic substitutes, forming hybrid DTs for real-time performance prediction, optimization, and control. This paradigm emphasizes cross-model feedback, UQ, and online adaptability.

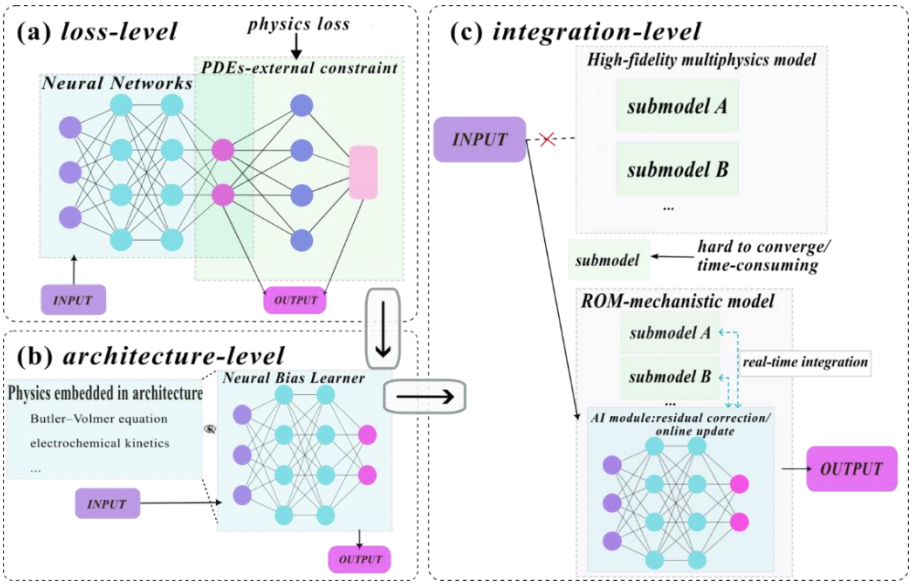

Figure 4. Hierarchical Framework and Evolution of PIAI in SOC Modeling. **(a)** Loss-level physics injection: Physics acts as a soft constraint via residual loss, suitable for inverse problems with sparse data; **(b)** Architecture-level fusion: Physics is embedded into network topology (e.g., hardwiring Butler-Volmer equations), enhancing interpretability; **(c)** Integration-level correction: Physics governs the interaction between mechanistic backbones and AI residuals, enabling robust DTs.

Beyond this hierarchical taxonomy, many SOCs-oriented PIAI studies exhibit hybrid characteristics spanning multiple levels of this hierarchy. For example, a model may employ loss-level residual penalties while simultaneously embedding mechanistic features as architectural priors, or extend an architecture-level hybrid into a system-level residual coupling. Rather than treating these as inconsistencies, this review classifies each work by its dominant functional role within SOCs modeling—whether it primarily constrains, embeds, or couples physics.

4. Applications of PIAI

PIAI methods in SOCs can be stratified by how and where physical knowledge intervenes in the learning process. At the loss level, physics acts as an external constraint, enforcing governing

equations through residual or boundary penalties. At the architecture level, physics becomes an internal structural prior, embedded in the network topology or feature flow. At the integration level, physics governs cross-mode interactions, coupling mechanistic solvers and data-driven surrogates within hybrid DTs systems. This three-tier taxonomy reflects an evolution from constraint→structure→interaction, each balancing fidelity, efficiency, and deployability. To facilitate cross-cutting retrieval, in addition to the depth-of- physics-integration taxonomy, we provide an application-oriented literature index (Table 2).

Table 2. Application-oriented Index of PIAI Studies in SOCs.

Application	Paper*	Representative Algorithms	Data Need Mirco	Cell/Stack
Field Reconstruction/Inverse Problem	[62–72]	PINN / cPINN, GAN, CNN	High	Medium/High
Parameter Identification/Calibration	[62–64,66,71,73–77]	Inverse PINN / B-PINN, DNN / ANN	Low	Low/Medium
Performance Mapping/Operation Optimization	[65–67,70,72–74,76,78–80]	PINN, GAN, DNN, CNN	High	Medium/High
Design Optimization	[13,65,69–80]	PINN, GAN, CNN	High	Medium
State Estimation	[63,66–68,70,72,81–83]	Inverse PINN, CNN, GAN, LSTM	High	Low/Medium
Online Control	[67,70,84]	PINN, Kalman Fliter	-	Medium

*Individual studies often span multiple tasks.

4.1. Loss-level physics injection

The foundation of PIAI lies in the loss-level injection paradigm, where physical knowledge is enforced externally through the optimization objective. In this setting, the neural network minimizes a composite loss comprising data-misfit terms, PDEs residuals, and IC/BC penalties, thereby constraining the solution space to obey conservation laws even under data scarcity (Figure 4a).

In early SOCs research, equation-based thermal and electrochemical models had already embodied this paradigm long before the emergence of modern PINN. Rauh *et al.* formulated finite-volume energy balance equations that described coupled heat conduction, gas enthalpy flow, and exothermic reaction enthalpy within SOFC stacks [85]. At a higher fidelity, Huang *et al.* and Bove coupled first-principles PDEs solvers with parameter estimation routines that explicitly penalized violations of energy and mass conservation in SOFC-gas turbine hybrid systems [86–88]. These works collectively established the loss-level injection mindset—treating physical consistency as an optimization constraint rather than an architectural property.

With the advent of PINN, this philosophy was generalized into a flexible learning framework. At the continuum scale, Laubscher *et al.* first validated this principle in coupled heat-mass-flow problems by embedding multi-species convection-diffusion-energy equations into the loss [62]. Comparing single- *vs.* separated-network PINN on a humidified 2D channel shows that dedicating networks to momentum, energy, and species improves conservation and accuracy versus CFD references and supports parametric surrogates with inlet vapor velocity as an input. This maps naturally onto SOC balance-of-plant and interconnect/channel design: humidification control, thermal management, and multi-species mixing in fuel/oxygen channels can be emulated with stable PINN surrogates, enabling rapid scenario analyses

without repeated meshing/CFD runs. Similarly, Jagtap and Karniadakis' conservative PINN (cPINN) introduced interface-flux matching terms to ensure strict mass and energy continuity across domains, directly addressing spectral bias and boundary discontinuity in multi-physics learning [88]. These developments collectively highlight that residual formulation—how PDEs and IC/BCs are normalized, weighted, and coupled—remains the primary determinant of stability and generalization in PIAI.

In electrochemical contexts, Chen *et al.* integrated a one-dimensional diffusion equation and electrochemical boundary conditions into the loss to predict cyclic voltammetry (CV) curves of disk electrodes without discretization [64]. The PINN reconstructed current-potential relations under sparse data and physically consistent constraints, enabling inverse estimation of diffusion coefficients and boundary fluxes. Extending to morphological dynamics, Tao *et al.* encoded transport-reaction PDEs for Ni redistribution in patterned Ni/YSZ anodes [66]. They integrate a Cahn-Hilliard-type phase-field formulation into a PINN to inversely identify interfacial thickness and mobility parameters from operando top-view images, thereby predicting Ni spreading and pinch-off dynamics in SOFC anodes (Figure 5). The inferred "apparent surface diffusion coefficients" are 3–4 orders of magnitude larger than conventional values. The results suggest that surface diffusion alone cannot explain the observed Ni evolution and provide a reusable image-driven PINN paradigm for phase-field parameter inversion.

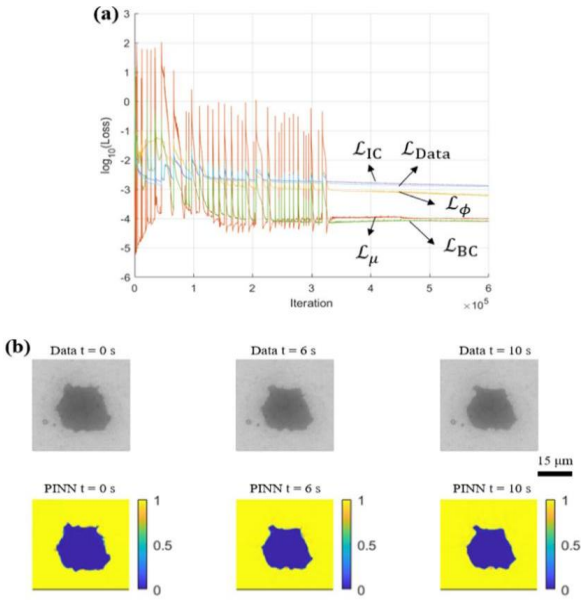

Figure 5. PINN prediction of Ni spreading in a patterned Ni/YSZ anode [66]. Reprinted with permission. Copyright 2024 Journal of The Electrochemical Society.

At the stack-level, Li *et al.* trained a PDE-constrained PINN surrogate on a two-dimensional SOFC model to generate steady-state performance maps, combining residual, IC/BC, and data-misfit losses [67]. A PINN surrogate aligned with a 2D high-fidelity multi-physics model is trained to rapidly generate performance maps and enable real-time set-point optimization; cell performance parameters are included as inputs to enhance generality. The surrogate attains a minimum voltage error of 0.513% with 0.5 ms per evaluation, and the maps delineate both peak-power loci and anode redox safety boundaries to track optimal conditions under degradation. This converts a high-fidelity model into a millisecond level tool for operations and optimization. Similarly, Yang *et al.* applied multi-condition PINN forindustrial-scale SOECs, producing efficiency safety maps that delineate feasible operation

windows (Figure 6) [70]. As the flow-field non-uniformity increased, the intersection between safe and efficient regions vanished—quantitatively capturing limits unreachable by empirical regression.

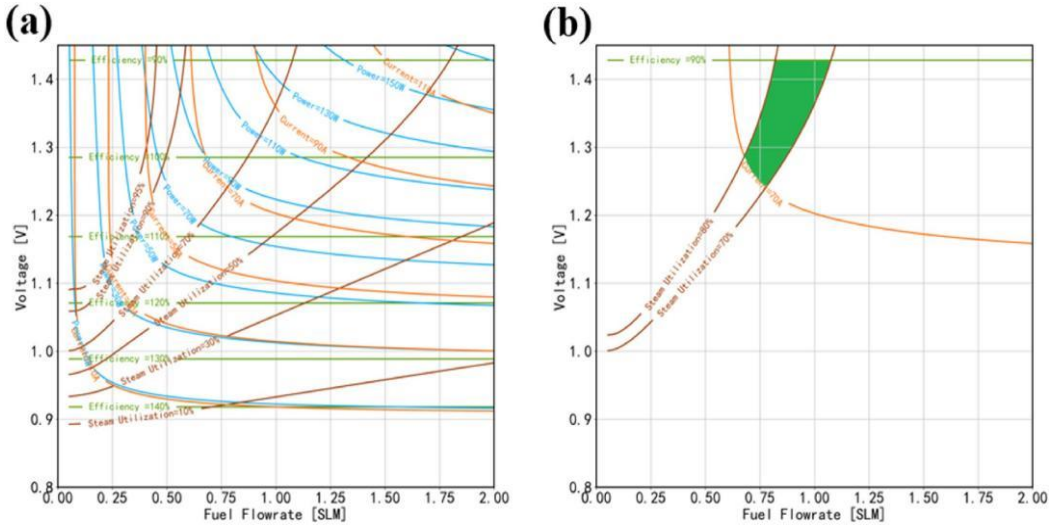

Figure 6. PINN-based prediction of safe and efficient operating regions of the SOEC under different fuel-electrode flow non-uniformities [70]. Reprinted with permission. Copyright 2025 International Journal of Hydrogen Energy.

Finally, Berardi *et al.* proposed an adaptive weighting scheme for multi-objective loss balancing among PDEs, IC/BC, and data terms, mitigating gradient competition and improving convergence across diffusion-reaction models [71]. The work introduces adaptive loss/gradient rescaling for inverse-PINNs that estimate parameters in diffusion and advection-diffusion-reaction models. The approach improves convergence and can jointly recover multiple parameters. In SOCs, where gas-phase transport through porous electrodes and supports governs polarization and local thermochemistry, such inverse tools are directly applicable to infer effective diffusivity, reaction rate constants, or mobile-immobile exchange parameters from spatial/temporal diagnostics, strengthening data-assimilative DTs.

Critical summary. Loss-level physics injection treats governing equations as soft constraints applied externally to the learning process. It is particularly effective for inverse and field-reconstruction tasks in SOCs, such as thermal-field estimation and parameter identification, where physical consistency outweighs data volume. However, its scalability remains constrained by spectral bias, gradient competition, and sensitivity to weighting. Emerging research—such as XPINN, FBPINN, and adaptive multi-fidelity residual learning—seeks to enhance convergence and generalization for large-scale SOCs stacks.

4.2. Architecture-level fusion

Architecture-level fusion represents a deeper form of physics-informed learning, where physical laws are embedded within the computational graph itself rather than enforced externally through penalties. Unlike loss-level injection, which constrains outputs post hoc, architecture-level fusion encodes conservation, constitutive, and coupling relationships directly into the network topology (Figure 4b). By aligning the neural architecture with governing equations or mechanistic surrogates, physical consistency becomes an intrinsic property of the forward pass. This transforms physics from a soft regularization signal into a

hard structural prior that shapes feature propagation, enhancing interpretability, sample efficiency, and stability under sparse or OoD data.

A clear precedent of this paradigm is the physically structured neural network proposed by Rauh *et al.* [90]. Derived from a quasi-linear energy-balance formulation, the architecture separates heat-transfer and exothermic-reaction subnetworks, introduces multiplicative coupling between temperature and current, and constrains the system matrix to a Metzler form (nonnegative off-diagonals, negative diagonals) to ensure thermodynamic stability. This design directly translates principles of energy conservation, stability, and locality into the network's connectivity. Earlier hybrid gray-box models—such as the Hammerstein and Wiener structures and LMI/interval-analysis-based control designs—also anticipated this fusion level by coupling linear dynamic kernels with nonlinear static mappings under explicit physical constraints [82,88]. Together, these studies laid the groundwork for physics-aware architectures that integrate analytic structure within neural representations.

At the microscale, Niu *et al.* developed the π-Learning framework for SOFC electrodes, where mechanistic descriptors—porosity, tortuosity, triple-phase-boundary density—were embedded as attention-guided branches jointly predicting electrochemical performance [65]. The resulting physics-informed GAN generated electrode microstructures whose current-density distributions matched both simulations and experiments (Figure 7), enabling controllable design under physical constraints. Similarly, Sciazko *et al.* used unsupervised image-to-image translation guided by conservation and microstructural evolution laws, achieving label-free prediction of Ni/YSZ aging trajectories—demonstrating that physical priors can steer latent representations without labeled data [68].

At the submodel level, Gnatowski *et al.* embedded a lightweight ANN module within the Butler-Volmer equation to dynamically learn the charge-transfer coefficient $\alpha(T, p_{H2})$ under varying thermal and gas conditions [73]. Instead of predicting voltage directly, the ANN operated as a functional node inside an electrochemical solver, updating kinetic parameters while preserving the physical form of the governing equation. The results show a significant reduction in the deviation between measured and modeled overpotentials, maintaining strong consistency even at previously unseen temperatures. Buchaniec *et al.* refined this "mechanism-as-backbone, learn-the-bias" design, constraining the surrogate to adjust only kinetic bias terms—achieving stable convergence and preserving reaction-diffusion consis-tency even with limited data [76]. The results demonstrate that, while ensuring physical consistency, the approach significantly accelerates the evaluation of local electrochemical terms, improving convergence and real-time performance in stack- and system-level simulations. Such formulations illustrate the essence of architecture-level PIAI: the network itself becomes a differentiable approximation of the physical process, maintaining local law compliance at every layer.

At the stack scale, Bao *et al.* first demonstrated hybrid reduced-order/PIAI architectures coupling mechanistic ROMs with embedded neural components within process-systems-engineering (PSE) toolchains [74]. While this study predated full integration-level coupling, it established the foundation for structural fusion between mechanistic surrogates and learning-based residual branches. Wang *et al.* extended this by embedding conservation and transport constraints in both loss and architecture, yielding hybrid gray-box models that replicated SOFC stack behavior across load transients [78]. Although physical supervision is introduced in the loss layer during model training, its main innovation lies in the embedding of physical prior structure within the network, and is therefore attributed to the architectural level. Olowu *et al.* further demonstrated geometry-operation co-optimization through physics-guided

dual encoders, linking structural design parameters to operational performance via a constrained latent manifold [13]. These systems illustrate how physics-aware topologies can support real-time prediction, parameter tuning, and controllable operation in complex SOCs stacks.

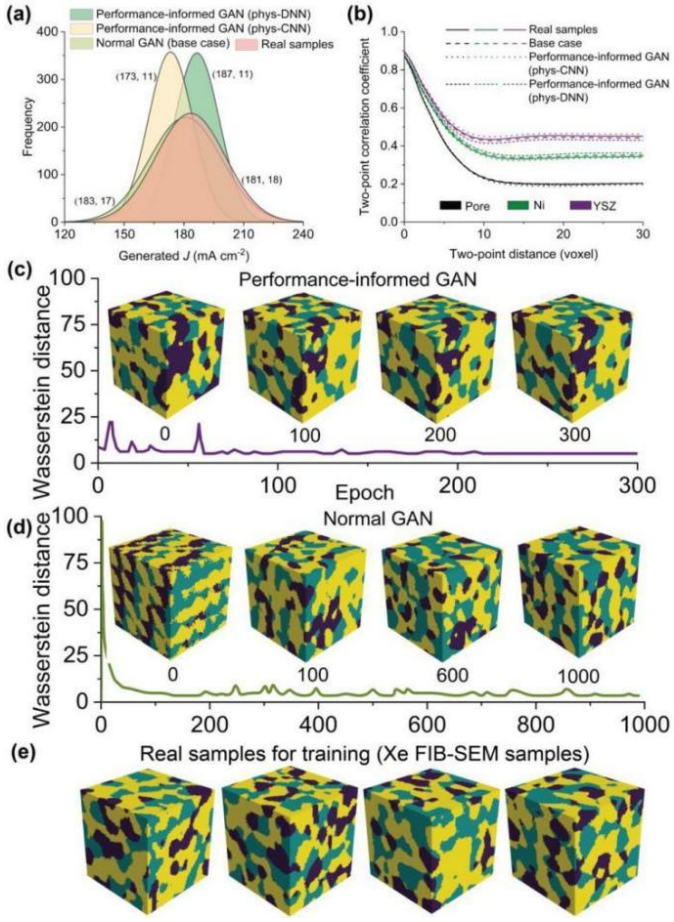

Figure 7. Performance-informed GAN generates electrode microstructures under physical constraints [65]. Reprinted with permission. Copyright 2023 Advanced Energy Materials.

At the diagnostics and health-monitoring level, Le *et al.* embedded electrochemical impedance spectra (EIS) features into physics-mapped latent spaces, constructing a self-consistent health index that preserved the impedance-reaction correspondence under in-situ conditions [63]. By forcing latent features to evolve along physically meaningful trajectories, this approach maintained causal interpretability across degradation stages—a hallmark of architecture-level PIAI in diagnostics. The results show consistency with experimentally measured EIS trends in short stacks. The confusion matrix for cross-condition classification exhibits over 90% accuracy along the diagonal, indicating clear distinguishability among the three fault types. The implication for SOCs is to transform stack-level EIS data into actionable state-of-health (SoH) indicators, fault classification labels, and degradation severity regression, thereby enabling a data-driven pathway for stack-level operation and maintenance as well as preventive diagnostics.

Collectively, these developments mark a transition from residual optimization (loss-level) to structure-level embedding, enabling interpretable and robust SOCs modeling under multi-physics coupling. By embedding governing laws, constitutive equations, or mechanistic surrogates directly into neural architectures, architecture-level fusion ensures internal physical consistency, enhances generalization under sparse data, and provides transparent pathways for interpretability and control.

Critical summary. Architecture-level fusion represents the middle tier of physics-informed learning. It translates physical knowledge into network topology, hardwiring physics into the information flow itself. Compared with loss-level injection, which treats physics as external supervision, or integration-level correction, which couples multiple models via feedback, this paradigm embeds governing relationships and physical submodels directly within the architecture. For SOCs, it excels in microstructure evolution, electrode kinetics, stack-level dynamics, and diagnostics by ensuring local physics compliance and interpretability at every layer. Future progress will likely focus on uncertainty-aware hybrid branches, physics-guided attention mechanisms, and transferable encoders that generalize across materials and operating conditions within physics-informed design spaces.

4.3. Integration-level correction

Integration-level correction represents the system-level embodiment (on the stack components) of physics-informed learning, where physical laws regulate the interaction between mechanistic and data-driven models. Rather than embedding physics inside a single network, this paradigm links interpretable mechanistic backbones—high-fidelity solvers or ROMs—with AI-based residual or surrogate modules through bi-directional residual exchange. Physics thus acts as an *interactive constraint* governing consistency, feedback, and correction across coupled modules.

In SOCs applications, this approach underpins DTs and control frameworks by enabling fast yet physically consistent surrogates for stack-level dynamics, thermal-mechanical stress, and degradation monitoring. Although methods such as those of [74] originated from architecture-level fusion, their evolution into multi-fidelity "base plus residual" stack qualifies them here, as their defining feature is cross-model residual coupling at the stack scale.

Integration-level correction represents the system-level embodiment of physics-informed learning, where physical knowledge is not merely embedded within a single neural network but governs the interaction between mechanistic and data-driven models across scales. This paradigm unifies high-fidelity solvers, ROMs, and learning-based compensators within a closed-loop residual-exchange architecture (Figure 4c). Here, physics continues to play an active role—not only as priors or losses, but as governing constraints that guide residual propagation, consistency enforcement, and adaptive correction across model hierarchies. Through this cross-model feedback, integration-level correction achieves a synergy of fidelity, efficiency, and adaptability that remains fundamentally physics-informed in spirit.

At the micro/electrode scale, Buchaniec *et al.* substituted the classical Butler—Volmer kinetics with a physics-regularized surrogate model constrained by thermodynamic losses, achieving over an order of magnitude improvement in computational efficiency while preserving thermodynamic consistency [75]. In a subsequent work, the authors introduced an architecture-level fusion strategy to correct the intrinsic deviation of the governing equations, and further replaced the entire dynamic sub-model with an artificial neural network (ANN), which can be categorized as an integration-level correction approach [76]. Campbell *et al.* introduced Gaussian-process surrogates for oxygen-exchange kinetics in LSCF, substituting equilibrium, rate, and diffusion sub-equations within a unified physics-guided surrogate that preserved reaction-transport consistency across regimes [77]. Focusing on the oxygen surface exchange and diffusion kinetics of the LSCF cathode, the authors developed a data-driven model to shorten calibration cycles and enhance predictive capability under high-temperature reduction and re-oxidation conditions. By integrating multi-source data with interpretable statistical and

machine learning methods, the study provides more reliable prior estimates of kinetic parameters for coupled SOC cathode simulations. Results indicate that the improved oxygen kinetics priors can be directly fed into cathode-limited multi-physics models, reducing the impact of parameter uncertainty on voltage and polarization decomposition. Unlike loss-level injection, these surrogates are reintegrated into the governing equations of the mechanistic solver, ensuring that learned corrections satisfy conservation laws and boundary flux continuity.

At the stack scale, Ba *et al.* constructed a hybrid mapping between mechanistic and full-physics models, using the former to generate state–source datasets that constrain an ANN to reconstruct nonlinear source terms while conserving energy and mass [80]. The resulting residual-informed surrogate achieved ± 2% accuracy and orders-of-magnitude speed-up—illustrating physics-informed residual exchange at the solver level. By formulating source terms (e.g., Faradaic sources and overpotential decomposition) and the governing equations for temperature and species distributions, current, temperature, and gas composition are selected as parametric inputs to train a two-layer NN for approximating the multi-physics solution. The results show that the method significantly accelerates the prediction of stack-level field distributions while maintaining physical interpretability, thereby supporting operating condition scanning and online evaluation. Bao *et al.* generalized this principle into a multi-fidelity framework where Kriging or ROMs supply physics-based priors, and deep networks learn systematic bias fields subject to physical regularization [74]. This "base plus residual" architecture realizes a data-efficient, constraint-preserving gray-box pipeline for SOFC optimization and feasible-domain construction.

Within the DTs context, Christopher *et al.* integrated PINN, UQ, and federated learning (FL) to create a thermo-mechanical monitoring loop where residual physics losses propagate between edge models and cloud solvers (Figure 8) [83]. The authors performed Bayesian calibration of parameters such as thermal expansion coefficients and elastic modulus, propagating uncertainty to analyze the sources of stress variance. A reinforcement learning (RL) approach was then used to dynamically adjust temperature profiles to reduce interfacial stress. Results show an 18% reduction in peak stress, a 32% decrease in temperature gradients, and a 60% reduction in voltage fluctuations. The estimated maintenance-related cost over five years is reduced by more than 30%, as demonstrated in the stack-level comparison table. Patel *et al.* proposed a gray-box model by combining mechanistic voltage equations (Nernst and polarization terms) with a neural network-based state submodel, which is embedded into a MPC framework to achieve constrained tracking and disturbance rejection for SOFCs. The NN is used to predict unmeasurable or difficult-to-measure internal states such as gas partial pressures, while the voltage is computed online using mechanistic equations. The control layer employs MPC to handle constraints and perform receding-horizon optimization. Results indicate that, compared to purely mechanistic or data-driven models, the gray-box MPC achieves a better balance among tracking accuracy, robustness, and computational efficiency, making it suitable for upper-level energy management and stack-level control [84]. A representative implementation of such a framework is shown in Figure 9, which details a case study of PINN-assisted MPC where physics constraints ensure real-time thermal management on embedded hardware.

At the degradation and lifetime scale, Prokop *et al.* parameterized long-term aging kinetics within gray-box ROMs, using mechanistic state evolution to constrain learning of slow-variable dynamics [81]. Based on synthetic and real (FIB-SEM) microstructures, the effects of initial TPB density, Ni particle size, and pore structure (including tortuosity and pore radius) on TPB evolution and overpotential were

systematically investigated. The results show that higher initial TPB density leads to better long-term stability; larger Ni particle sizes accelerate TPB degradation and increase overpotential; reducing tortuosity and increasing pore radius improve diffusion and enhance terminal voltage, consistent with trends observed in stack experiments. Wu *et al.* assimilated electro-chemo degradation in PCFCs through physics-regularized surrogate submodules, which absorbed unresolved coupling terms while maintaining field consistency [82]. A degradation root-cause analysis framework based on "interfacial electrochemical coupling" is proposed for PCEC (a member of the SOC family), elucidating the failure mechanisms at the electrode/electrolyte interface and offering material and structural strategies. By integrating electric field distribution, chemical potential gradients, and interfacial migration/phase transformation behaviors, the authors established a causality chain that is validated by experiments. The results reveal that interfacial electrochemical coupling can trigger localized stress and phase reconstruction, thereby accelerating performance degradation; optimizing interfacial band alignment/doping and the interlayer transition zone can significantly suppress these effects. Analogous strategies have appeared in porous-media systems: Delpisheh *et al.* implemented hybrid inversion and data assimilation loops where residual updates are constrained by PDE-based physical priors—directly paralleling the SOCs degradation-twin architecture [69]. The authors review the applications of ML in modeling, inversion, and acceleration within porous media, covering methods such as PNM, ROM, PINN, Kriging, and XGBoost. This framework is summarized as a general-purpose ML toolbox for SOCs electrodes—typical porous composites—enabling a "from pixel to property" pipeline that integrates seamlessly with microstructure reconstruction, phase-field modeling, and system-level ROM.

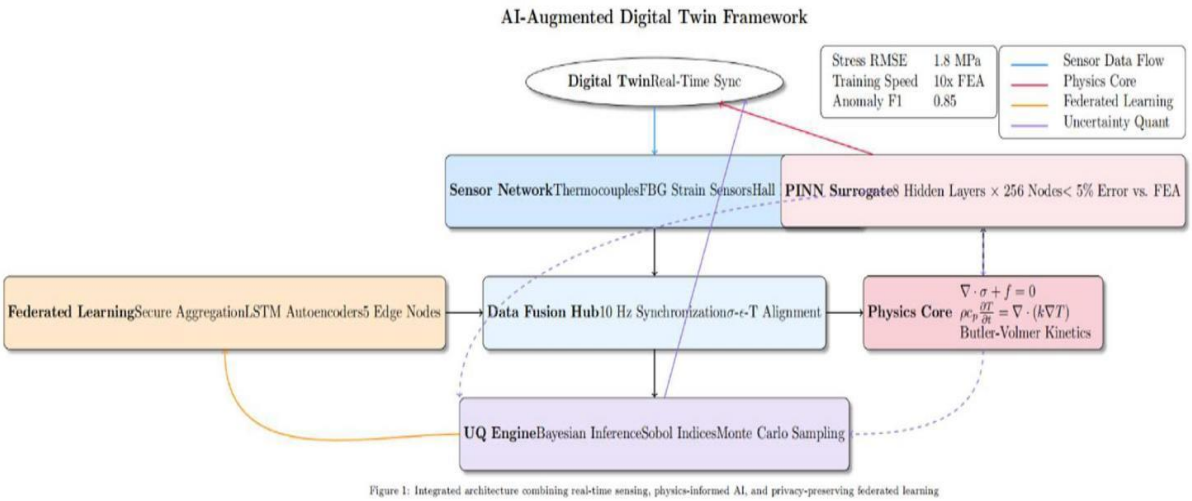

Figure 8. Integration-level physics-informed DTs framework for SOFC thermo-mechanical monitoring [83]. Reprinted with permission. Copyright 2025 Ceramics International.

Critical summary. Integration-level correction constitutes the highest tier of physics-informed coupling—embedding physics not within a single learner but throughout a network of interacting models. By enforcing residual and conservation consistency during cross-model communication, it transforms PIAI from model-centric learning to stack-level orchestration, balancing interpretability, adaptability, and deployability for SOCs DTs. Ultimately, this paradigm preserves the core tenet of PIAI: physics remains the governing signal that regularizes, constrains, and validates learning across scales and modules.

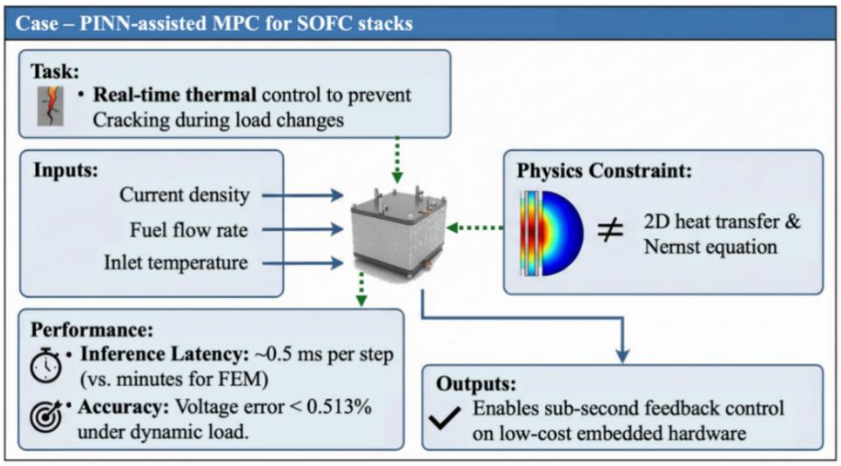

Figure 9. Case study of a PINN-assisted Model Predictive Control (MPC) framework for SOFC stacks. The schematic details the input variables, embedded physics constraints (e.g., 2D heat transfer equations), and the resulting millisecond-level inference capabilities (~0.5 ms) that enable real-time thermal management on embedded hardware.

To provide a concrete engineering perspective on the deployment of these frameworks, Table 3 summarizes the typical computational benchmarks across different PIAI paradigms. The data highlights the characteristic 'training-for-inference' trade-off: while training high-fidelity surrogates may require significant GPU resources and thousands of epochs, the resulting models achieve millisecond-level inference latencies, making them viable for real-time DTs and onboard control.

Table 3. Quantitative Benchmarks of Representative ML/PIAI Models for SOCs.

Category	PINN Surrogate Model [67,108]	PINN Reverse/Low Data [71]	PINN/DT [83]	Traditional DNN/ML (comparison) [78]
Data Size	50,000 simulation cases (generated from 2D multiphysics models)	< 40 data points (for training); 100 spatial points * 100 time points	10,000 COMSOL simulations + 500 *in situ* strain measurements	> 8,000 to 20,000 cases (for ROM/classifier)
Training Time	~1.5 hours (per run)	~800 seconds (5000 epochs); ~1000 seconds (10000 epochs)	Simulation speedup increased by 90% (from 8.2 hours to 0.8 hours).	3.72 s (ANN Regression); 43,382 seconds (Complex Hybrid CNN-NARX)
Hardware	NVIDIA RTX GPU (24 GB), Intel Core i9 CPUs, 36 GB RAM	Apple Silicon M1 Pro processor (10 cores, 16 GB RAM)	NVIDIA A100 GPU (40GB VRAM), Intel Xeon Platinum 8380, 512 GB DDR4 RAM	Single GeForce RTX 3090 GPU
Inference Time	~0.5 ms per case	-(The model is used for parameter inversion)	10 times faster than 3D FEA	~0.5 ms (NN surrogate model); ~5 s (2D physics model)
Core Application	Performance Mapping	Diffusion/transport parameter identification	Thermomechanical stress prediction and degradation monitoring	Performance prediction, fault classification

5. Challenges, limitations, and outlook

5.1. Challenges and limitations

For SOCs—a prototypical multi-scale, multi-physics, strongly coupled system—PIAI first confronts a structural challenge of trainability and spectral bias: although classical PINN leverage physical constraints

to improve data efficiency in small-sample and inverse settings, their training dynamics favor low frequency modes, leading to loss of detail in high-gradient regions such as reaction-diffusion boundary layers, interlayer coupling zones, and local thermal hot spots. Consequently, even as the aggregate loss decreases, one may observe local conservation satisfied yet global deviation persists [92]. Two principal avenues have emerged to mitigate this issue. First, enhance representation capacity—introduce random Fourier features or positional encoding at the input and adopt sinusoidal-activation architectures such as sinusoidal representation networks (SIREN) to explicitly capture oscillatory solutions and their higher-order derivatives. Second, reshape the optimization landscape—employ neural tangent kernel (NTK)-based adaptive loss reweighting and spatio-temporal domain decomposition (cPINN/XPINN) to partition geometric complexity and stiffness. Both families of methods have demonstrated efficacy on generic PDEs and engineering benchmarks [89,93–95]. Nevertheless, theoretical analyses of XPINN and parallel domain decomposition indicate that domain partitioning introduces a generalization-efficiency trade-off; recovery of high-frequency content and stable extrapolation remain bottlenecks for multi-mechanism coupled systems such as SOCs. A robust pipeline should therefore advance along three coordinated fronts—representation, training, and architecture [96,97].

The second core bottleneck concerns multi-fidelity data fusion and OoD generalization: experimental and in-service data are sparse and noisy, whereas simulation data are abundant yet exhibit systematic bias. Naive concatenation tends to become unstable near operating-condition boundaries and in extrapolation regimes. Accordingly, one should either (i) explicitly learn the nonlinear mapping from low fidelity to high-fidelity as a supervised target, or (ii) perform residual correction around a physics-based/ROM backbone to estimate the error field between the ground truth and the backbone prediction [98]. In the SOCs domain, engineering-ready progress has emerged: a PINN-centered performance map guided by a two-dimensional multi-physics model reduces errors in key SOFC outputs to engineering-grade accuracy and enables millisecond-level inference, thereby supporting online optimization and parameter tuning [67]. For industrial-scale SOECs, physics-constrained approximations and surrogate models likewise enable time-efficient, sample-efficient optimization with only a small number of high-fidelity samples, offering a deployable paradigm for large-scale operations-and-maintenance scenarios [70]. Meanwhile, multi-fidelity Bayesian neural networks (MF-BNNs) facilitate cross-domain transfer by yielding predictive distributions with calibrated credible intervals and explicit risk labeling, thereby reducing dependence on high-fidelity data while preserving interpretability and robustness [99]. Third, the deployment of ML models in scientific and engineering systems, such as SOFCs, confronts the critical risks of OoD inputs and model drift. Purely data-driven black-box models typically perform well only within the domain covered by their training data. Their generalization capability is often limited during extrapolation or when encountering unseen operating conditions, potentially leading to physically inconsistent or unreliable predictions. Deep learning (DL) models, in particular, are prone to making high-confidence errors when input patterns deviate significantly from the training distribution. For instance, a PINN surrogate for SOFCs may exhibit a significant decline in prediction accuracy when the current density exceeds its training range (e.g., > 1.5 A/cm^2). Furthermore, model drift arises when the distribution of real-world data diverges from the training data over time due to dynamic environmental changes or equipment aging. In high-temperature systems like SOFCs, long-term degradation mechanisms—such as Ni coarsening—alter system dynamics, rendering the initially trained model inaccurate [100].

Third, deployment confronts the critical risks of OoD inputs and model drift. Purely data-driven models often lack generalization during extrapolation or system degradation, leading to physically inconsistent predictions. To ensure robust operation for high-stakes decisions, a transition from prediction accuracy to reliability is required through three integrated strategies: (i) Reinforced Monitoring and UQ: Explicitly quantifying uncertainty assesses trustworthiness. Methods like Bayesian PINNs (B-PINNs) [101] mitigate overfitting and return posterior uncertainty, while Conformal prediction generates theoretically guaranteed prediction intervals and "out-of-spec" alarms for time-series data [102,103]. (ii) Uncertainty-Aware Control: In closed-loop systems like MPC, real-time uncertainty estimates should be propagated into the cost function. This prompts the controller to adopt conservative strategies by penalizing states with high uncertainty. (iii) Physics-Embedded Fallbacks: Hybrid architectures should employ mechanistic models as reliable backbones. Strategies such as physical operability checks (filtering infeasible inputs) or residual correction ensures that if the AI component fails due to drift, the system reverts to the robust physical core, maintaining safety boundaries.

Fourth, microstructure-resolved, cross-scale DTs are constrained by the cost of 3D/in-situ imaging and the scarcity of temporally paired datasets, making quantitative mapping from microscopic evolution to macroscopic degradation—and cross-material transfer—challenging; physics-consistent image learning and multi-physics coupling are therefore required [69]. For Ni/YSZ electrodes, physics-constrained unsupervised image learning—embedding conservation laws and dynamics into unsupervised image-to-image translation (UNIT)—has successfully predicted morphological evolution during the NiO→Ni reduction using unpaired, small-sample datasets, substantially alleviating the annotation bottleneck [68].

On the other hand, phase-field-informed PINN inversion can estimate key parameters—such as interfacial thickness and mobility—from operando images, thereby establishing a route to close the loop among images, parameters, and performance/lifetime [66]. A recent review of SOCs-oriented DTs further emphasizes the need for reproducible experimental standards and unified evaluation protocols across reconstruction, descriptor generation, and multi-physics simulation to support cross-material and cross-temporal transfer and reuse.

Fifth, stack-level diagnosis and observability remain challenging: stack EIS reflects a composite response from many cells and is affected by flow-field distribution, parasitic inductance, and perturbation/excitation conditions. As a result, equivalent-parameter separation and mechanistic attribution are often not robust, motivating a simulation-informed spectroscopic learning pipeline developed in tandem with UQ [104]. A simulation-informed diagnosis strategy—training classifiers on EIS datasets of multiple failure modes generated by short-stack simulations and validating them with experimental measurements—has demonstrated cross-condition identification capability and provides a template for deployable in-service health monitoring.

SOCs pose modeling and diagnosis challenges that current AI methods only partly solve. Standard PINN-style models can miss sharp local features, and mixing sparse, noisy experiments with biased simulations often breaks down near operating limits. Reliable use in control needs simple, trustworthy uncertainty estimates, which are still maturing. At the microstructure and system levels, limited imaging data and blended EIS signals hinder clear attribution, though physics-guided image learning and simulation-informed diagnostics are promising; consistent datasets and benchmarks are still needed.

5.2. Outlook

Building on the identified challenges and opportunities, we outline a cohesive roadmap for the future of PIAI in SOCs.

5.2.1. Operating condition reconstruction and field estimation

In adjacent electrochemical systems, PIAI techniques have shown great promise in estimating internal operating conditions (temperature, stress, species concentrations) that are challenging to measure directly. For example, in lithium-ion batteries, researchers have integrated physical heat equations into neural networks to predict internal temperature distributions with high accuracy, using the governing thermal dynamics as a regularization for the model [105]. Similarly, a hybrid PINN approach by Pang *et al.* incorporated a simplified electrochemical model (a single-particle model with thermal dynamics) into a Bi-LSTM network, enabling accurate estimation of the battery's heat-generation rate under dynamic loads [106]. These methods are effective because they enforce consistency with known physics (e.g., energy conservation, diffusion laws) while leveraging data-driven learning, thereby reconstructing full-field profiles from limited sensor inputs. In the fuel cell domain, Kang *et al.* demonstrated that PINN can solve for complex coupled fields (e.g., water saturation distribution in a PEM fuel cell under flooding conditions) orders of magnitude faster than CFD, without requiring labeled data for the field of interest [107]. This ability to infer spatially-resolved conditions stems from embedding the multi-physics PDEs (mass, momentum, heat transport) into the neural network's loss function, yielding physically plausible field estimates even with sparse measurements.

Transferring these approaches to SOCs could significantly advance SOCs diagnostics and control. Physics-informed surrogates could reconstruct critical internal states like fuel/oxidant concentration gradients or temperature/stress distributions across an SOCs stack, using only surface measurements (e.g., voltages, limited thermocouples) as inputs. For instance, a PINN trained on SOCs thermal-fluid equations might infer the 3D temperature map through a cell during operation, helping identify hot spots or thermal gradients that arise under high current densities. Such field reconstruction would be invaluable for addressing SOCs-specific challenges: redox cycling can induce localized re-oxidation of the anode, and sulfur poisoning can cause non-uniform reaction rates—both phenomena could be detected early by observing anomalous spatial patterns in estimated temperature or gas concentration fields. In essence, PIAI could act as a virtual sensor network for SOCs, providing real-time insight into internal conditions (e.g., electrode utilization, stress hotspots) that are otherwise inaccessible, and enabling timely mitigation strategies to protect the cell.

5.2.2. Materials and kinetic parameter inference

Another promising direction is using PIAI to infer difficult-to-measure material properties and kinetic parameters in energy devices. In the battery field, PINN have been developed to automatically calibrate electrochemical model parameters (e.g., diffusion coefficients, reaction rate constants) by training the network to satisfy the model's differential equations alongside experimental data. Wang *et al.* employed three parallel PINN to identify multiple lithium-ion cell parameters simultaneously, leveraging the known battery physics to constrain the search space and achieve accurate parameter estimates from routine

charge-discharge curves [108]. In proton-exchange membrane fuel cells, data-driven strategies augmented with physics have emerged for parameter estimation as well. Salem *et al.* introduced a reinforcement learning approach that treats the fuel cell model as an environment; the RL agent learns to adjust kinetic parameters (e.g., membrane resistance, exchange current densities) to minimize error between simulated and observed voltages, outperforming traditional optimization in capturing the proton-exchange membrane fuel cell (PEMFC)'s nonlinear dynamics [109]. The effectiveness of these approaches comes from their hybrid nature: by blending machine learning with the structure of physical models, they can deduce parameters with far fewer experiments, all while ensuring the inferred values remain physically realistic (e.g., positive diffusivities, reasonable activation energies).

Adapting such methods to SOCs research could greatly accelerate materials development and model validation. SOCs involve many uncertain properties-oxygen ion diffusivities in ceramics, electrode triple-phase boundary kinetics, interface contact resistances—that traditionally require lengthy testing to determine. A PIAI could assimilate routine performance data (like IV curves or EIS spectra) and identify which parameter values make an SOCs model best match the observations. For instance, one could integrate SOCs reaction-diffusion equations into a PINN and treat the sulfur poisoning rate constant or anode porosity as learnable parameters; by training against measured degradation data, the network would converge on values that explain the performance loss. This approach would allow *in situ* updating of model parameters as the cell ages (tracking, say, a drop in oxygen diffusivity due to pore clogging). It also aids fundamental understanding: if a model with physics-informed learning reveals an anomalously fast drop in surface exchange coefficient after redox cycles, it indicates that interfacial reactivity is decaying, guiding researchers to investigate that mechanism. In summary, PIAI-based parameter inference can serve as a powerful digital lab assistant for SOCs—rapidly tuning complex models to new materials or operating conditions and even detecting subtle changes (e.g., onset of poisoning) through the lens of parameter shifts.

5.2.3. Lifetime and degradation-aware modeling

Machine learning is increasingly used to predict device lifetime, and incorporating physics into these models yields robust, extrapolative predictions. In the battery arena, for example, Wang *et al.* developed a PINN for lithium-ion SoH prognostics that combines empirical degradation laws with neural networks [108]. Their model encodes known capacity fade behavior (e.g., growth of solid-electrolyte interface) into the network structure, enabling accurate SoH predictions across 387 cells under diverse conditions while maintaining physical plausibility in extrapolation. In the fuel cell domain, Ko *et al.* formulated a PINN to prognosticate PEM fuel cell remaining useful life, embedding mechanistic degradation equations (for catalyst activation loss and membrane ohmic loss) into the learning process [110]. This physics-guided model could predict long-term voltage decay trajectories more stably than purely data-driven LSTM benchmarks, even when training data were limited. Beyond PINN, hybrid modeling is being explored for degradation: Polo-Molina *et al.* introduced a coupled-model approach for PEM electrolyzers where one ODE represents membrane thinning and another captures voltage rise; a neural network is trained to satisfy both, yielding a highly interpretable predictor for long-term performance loss under various stressors [111]. By fusing domain knowledge (e.g., first-order degradation kinetics) with learning, these models can capture nonlinear aging trends and sudden failure modes that black-box models might miss.

For SOCs, which face complex degradation phenomena, physics-informed prognostics could be transformative. SOCs suffer from processes like Ni coarsening, chromium poisoning, and redox-cycle damage that evolve over thousands of hours. A PIAI framework could incorporate these known failure modes into a prognostic model—for instance, including a term for anode porosity loss per redox cycle or a sulfur coverage fraction that poisons the catalyst, and train on long-term test data to calibrate any unknown rates. The result would be a degradation-aware DTs of the SOCs that can predict capacity or efficiency decline under arbitrary duty cycles. Importantly, such a model would not only forecast end-of-life, but also provide insight why performance is dropping: e.g., it might attribute a rapid voltage decay to escalating anode polarization resistance, signaling sulfur deposition. This physics-informed clarity is crucial for devising mitigation: if the model indicates oxide scale growth at the interconnect is the life-limiting factor, one can focus maintenance or materials changes there. Additionally, because these models embed fundamental conservation laws and mechanistic patterns, they are likely to generalize better when extrapolating to new SOCs designs or operating regimes. In summary, embedding degradation physics into AI models could enable reliable lifetime predictions for SOCs stacks, while elucidating the dominant aging mechanisms—a key step toward proactive degradation management in real-world applications.

5.2.4. PIAI-assisted control, fault detection, and MPC

Adjacent fields also illustrate how PIAI can enhance control strategies and fault diagnostics for energy systems. In battery management, researchers have used hybrid models to improve early fault detection—for instance, Chen *et al.* integrated multiple physics-based electrochemical features (e.g., voltage relaxation metrics tied to lithium plating) into a machine learning classifier to detect the onset of lithium plating events that pure data-driven methods struggled to identify [112]. The study proposes a mesh-free PINN constrained by diffusion equations and electrochemical boundary conditions to simulate cyclic voltammetry on disk (1D), microband (2D), and square electrodes. The PINN-generated current-voltage responses agree closely with finite-difference/analytical solutions and quantify edge-induced current non-uniformity for square geometries. This offers a concise modeling route for higher-dimensional voltammetry while reducing the discretization burden of traditional numerical schemes. Likewise, Firoozi *et al.* demonstrated that augmenting machine learning with fractional-order impedance models can markedly improve detection of incipient battery faults: their approach merged a fractional physics model (capturing charge-transfer and diffusion dynamics) with a learning algorithm, successfully diagnosing internal short-circuits that eluded standard integral-order models [113]. On the control side, physics-informed neural surrogates are being deployed to enable fast, optimal control. Pozzi *et al.* trained a neural network to approximate a high-fidelity electro-thermal battery model, then embedded this surrogate in a model predictive controller for fast charging [114]. The surrogate preserved key physical behaviors (thermal limits, electrochemical constraints) by training on simulation data, allowing the MPC to compute optimal charge profiles in real-time without violating safety limits. Such PIAI-enhanced controllers marry the speed of learned models with the trustworthiness of physics, making them well-suited for safety-critical tasks.

By applying these concepts to SOCs, we can envision significant improvements in operational control and safety. For example, SOFC often need tight control of fuel utilization and temperature to avoid thermal stress or fuel starvation—a task complicated by their slow dynamics and multi-input nature. A

physics-informed ROM of an SOCs (learned from a detailed stack model) could serve as the core of a predictive controller that anticipates temperature spikes or fuel depletion and adjusts flows proactively. Because the model encodes SOCs thermodynamics and electrochemistry (e.g., Nernst potential variation with fuel concentration), the controller can enforce constraints like avoiding quick ramp rates that would overshoot thermal gradients. In terms of fault detection, SOCs stacks could benefit from algorithms that monitor for signatures of degradation or failure using physical insight. As an analogy to lithium plating detection, an SOCs-focused method might use voltage oscillation patterns or impedance shifts that correlate with sulfur accumulation at the anode and feed those into an ML model trained to flag sulfur poisoning early. Similarly, pressure drop or temperature distribution anomalies (features derived from physical models of the SOCs balance-of-plant) could be inputs to a physics-informed diagnostic tool to detect cracking in an electrolyte or sealing failure in a stack. The combination of model-based features with data-driven classification can sharply reduce false alarms and improve sensitivity, as seen in batteries. Ultimately, PIAI-assisted control and diagnostics for SOCs promises more robust operation: the system would not only respond to deviations more intelligently (thanks to its internal physics-aware model), but also provide explanations for alarms (e.g. "Cell 3 likely experiencing fuel starvation") that help operators take targeted corrective action.

5.2.5. Multi-scale coupling and DTs frameworks

A grand vision emerging in related domains is the DTs: a virtual replica of the device that fuses multiscale physics models with real-time data. Battery researchers, for instance, have begun developing DTs frameworks that connect microscale phenomena to pack-level behavior through AI. Shabeer *et al.* review how integrating multi-physics models with machine learning enables live tracking of battery state across scales—from electrode particle-level SEI growth up to pack-level thermal management—all synchronized with sensor data via cloud-edge computing [115]. Such systems employ hierarchical modeling: high-fidelity models or experiments generate a rich dataset of internal states, and then an AI surrogate (often informed by physics) learns to predict those states under new conditions instantaneously. This surrogate can be nested into a larger system model, yielding a composite that spans multiple scales yet runs in real-time. For example, researchers have trained deep neural operators on detailed 3D electrode simulations so that the DTs can predict spatial concentration and stress profiles in any new battery geometry on the fly [116]. By preserving physical structure (e.g., respecting conservation laws at each scale interface) in these learned components, the DTs remain grounded and interpretable. In fuel cells, similar ideas are taking shape: self-adaptive DTs have been proposed that use diagnostic data to update a PEM fuel cell's multi-physics model in real-time, adjusting parameters as the cell ages to maintain accuracy in performance prediction [117]. The power of these approaches lies in coupling phenomena that were previously treated in isolation—marrying, say, a catalyst microstructure degradation model with a macroscopic CFD model via an AI intermediary—so that the whole system can be simulated and optimized holistically. To guide researchers in navigating these complexities, Figure 10 provides an actionable checklist for addressing critical challenges in physics-informed SOC modeling, covering spectral bias, data fusion, and uncertainty quantification.

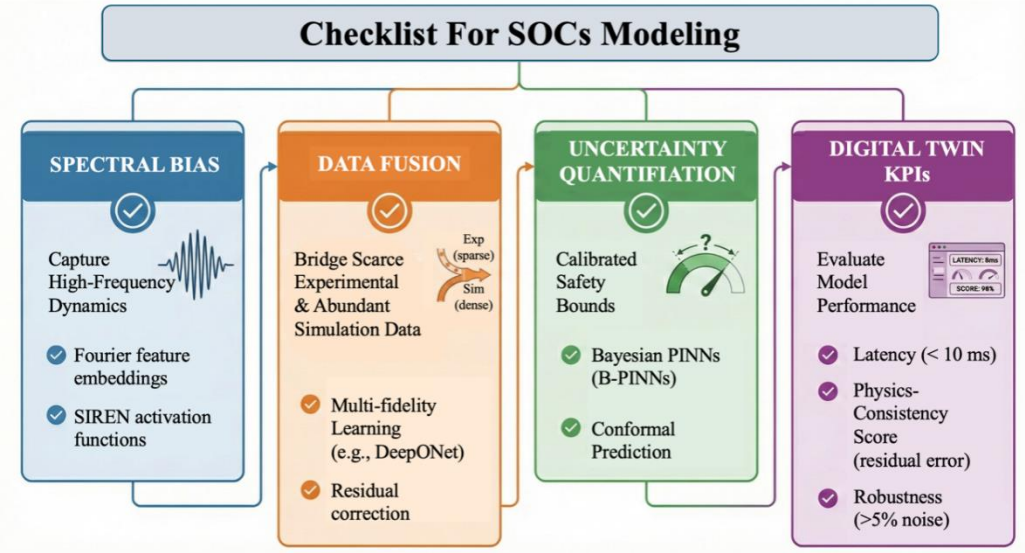

Figure 10. An actionable checklist for addressing critical challenges in physics-informed SOC modeling. The framework outlines specific strategies to mitigate spectral bias, fuse multi-fidelity data, and quantify uncertainty, while establishing standardized Key Performance Indicators (KPIs) for robust digital twin deployment.

Translating this to solid oxide technology, one can foresee comprehensive SOCs DTs that integrate everything from microstructural evolution to stack-level thermal-fluid dynamics. An SOCs operates across vast scales: nano-scale catalyst interfaces, porous electrodes, single cells, and full stacks with hundreds of cells and complex heat exchangers. PIAI can act as the glue between these layers. For instance, a multi-scale SOCs twins might include a microscopic model of electrode grain growth or poisoning (to predict how anode active surface area declines), which feeds its output into a cell-level electrochemical model. Instead of solving the grain growth PDEs inside the real-time simulator (which would be infeasible), one could train a neural network on offline microstructure simulations to rapidly predict the effect of, say, 100 redox cycles on porosity and conductivity—essentially a learned micro-scale model. This network, constrained by physical limits observed in the training data, would then update the cell model's parameters on the fly. Meanwhile, at the macro scale, a reduced-order thermal model of the SOCs stack could be continually corrected by sensor data via an AI filter, ensuring the DTs reflect the true stack temperatures and stresses. By coupling these components, the SOCs DTs would enable scenarios such as what-if analyses (e.g. "How would introducing H_2S for 10 hours impact long-term performance?") and real-time control optimization across the entire system. Importantly, because the twins is grounded in physics, it can extrapolate beyond previously seen conditions with more confidence than a purely data-driven model. The result is a powerful framework for both research and operations: SOCs designers could use DTs to test multi-scale design tweaks virtually, and plant operators could use them to predict and prevent failures (for example, forecasting that a certain load profile will lead to hotspot formation in the stack after 500 hours). By learning from successes in batteries, fuel cells, and other domains, SOCs researchers can leapfrog toward such integrated, AI-enhanced multi-scale models—paving the way for more resilient and optimized SOCs systems in practice. For practical implementation, Figure 11 summarizes typical hyperparameters and multi-stage training strategies specifically tailored for establishing robust physics-informed models.

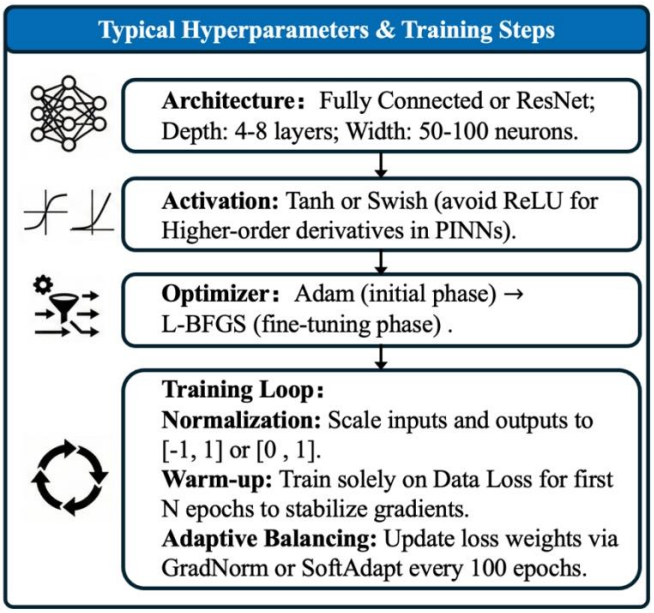

Figure 11. Typical hyperparameters and Training steps. The picture summarizes the recommended hyperparameters and multi-stage training strategies (e.g., activation functions suitable for high-order derivatives) specifically tailored for physics-informed modeling.

6. Conclusion

This review interrogates the long-standing tension between high-fidelity yet costly mechanistic modeling and fast but brittle data-driven learning for SOCs, and synthesizes a deployment-oriented, layered paradigm of PIAI. We advance a three-tier framework—loss-level physics injection, architecture-level fusion, and integration-level correction—that traces a "constraints→structure→interaction" progression. This taxonomy unifies previously heterogeneous efforts across microstructural evolution, stack-level performance mapping, and system-level diagnostics/control, and provides a practical scaffold for closed-loop DTs in engineering settings.

In terms of scope and fit: loss-level injection (e.g., PINN) imposes PDE residuals and IC/BC conditions as soft constraints and is well suited to field reconstruction and inverse problems under sparse data (e.g., temperature/concentration estimation, parameter identification, feasible-domain mapping). Architecture-level fusion embeds mechanistic features or simplified submodels directly into the network topology, converting "physics" into hard priors; it excels in small-sample regimes, cross-scale/crossfidelity fusion, and interpretable diagnostics. Integration-level correction couples an interpretable mechanistic backbone with data-driven residuals/surrogates, leveraging multi-model residual exchange and consistency constraints to jointly achieve real-time performance and trustworthiness—a pivotal pattern for maintainable SOCs DTs and MPC. The overall architecture of this deployment-oriented paradigm is depicted in Figure 12, illustrating the closed-loop data flow from sensor acquisition to the physics-informed digital twin core and final control actuation.

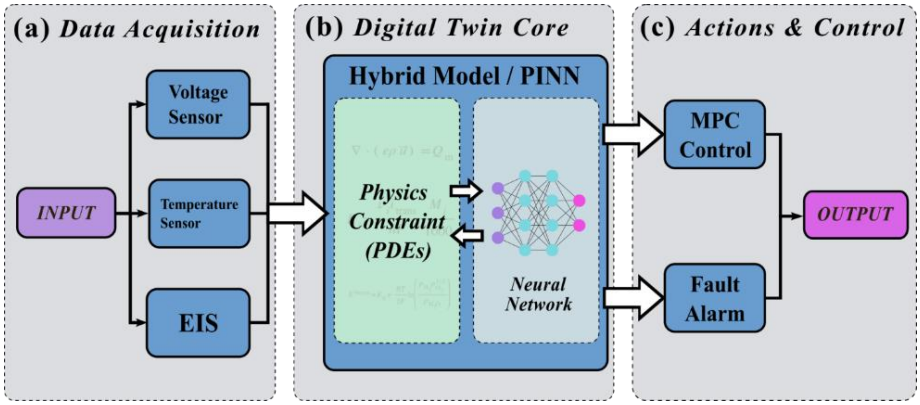

Figure 12. A closed-loop data flow from sensors to physics-informed DTs and control actuation. **(a)** Data Acquisition: Real-time assimilation of multi-source sensor measurements (e.g., voltage, temperature, EIS) provides the observational basis for the twin; **(b)** Digital Twin Core: The hybrid engine couples mechanistic governing equations (PDEs) with neural networks to reconstruct unobservable internal states and dynamic fields; **(c)** Actions & Control: Physics-consistent state estimates drive robust model predictive control (MPC) and proactive fault diagnosis to optimize system output.

For engineering deployment, we recommend key KPIs emphasizing latency, physics-consistency scores, and generalization robustness, following a workflow of high-fidelity priors→reduced-order/operator learning→UQ→closed-loop control/decision. High-fidelity models and principled experimental design provide supervisory priors; ROMs/operator surrogates (e.g., FNO, DeepONet) are trained to honor conservation and boundary consistency; systems then proceed under UQ and risk-aware safeguards into optimization and MPC; finally, in-operation data continuously calibrate DTs for lifecycle awareness and online adaptability.

We also identify several persistent, field-wide bottlenecks. (i) Spectral bias and stiff multi-physics coupling can omit boundary-layer and high-gradient details, calling for coordinated advances in representation (positional encodings/sinusoidal activations), training (adaptive weighting, domain decomposition), and architecture. (ii) Multi-fidelity fusion and OoD robustness remain fragile; robust patterns include low→high-fidelity mappings or mechanistic backbones plus residual correction. (iii) Inverse problems and UQ are prerequisites for control; Bayesian PINN and conformal prediction can provide calibrated intervals and violation alerts. (iv) Microstructure-to-macro performance linkages and EIS-based diagnostics are constrained by paired datasets and reproducible baselines, motivating standardized data protocols and replicable experiment–simulation pipelines.

Looking forward, we anticipate three complementary thrusts. Near term, establish open benchmarks (e.g., 3D thermal-field reconstruction, parameter identification, feasible-domain mapping) and reporting standards (ablation/UQ plus safety constraints). Midterm, validate gray-box DTs with safety-aware MPC in 5–20 kW demonstrators, using dual metrics of physics consistency and end-to-end latency. Long-term, realize microstructure-resolved, cross-material-transferable, adaptive SOCs DTs that enable predictive maintenance, lifetime management, and multi-objective optimal scheduling. In sum, PIAI is emerging as a unifying paradigm that bridges credible mechanistic knowledge and efficient learning; with continued progress in interpretability, UQ, and systems integration, it can underpin trustworthy, real-time, lifecycle-aware SOCs engineering.

Acknowledgments

This work was supported by the National Key R&D Program of China (2024YFB4106400), the Strategic Priority Research Program of the Chinese Academy of Sciences (XDA 0400000), the Science and Technology Commission of Shanghai Municipality (23DZ1201803) and the Fundamental Research Program of Industrial Foundation (SINAP-CYJJ-202502).

Author s' contribution

Conceptualization, Y.Z., M.Z. and C.G.; investigation, Y.Z. and M.Z.; data curation, Y.Z., M.Z. and Z.L.; writing—original draft preparation, Y.Z.; writing—review and editing, C.G., F.D., S.L., and Z.L.; visualization, Y.Z. and M.Z.; project administration, C.G. and S.L.; funding acquisition, J.W. All authors have read and agreed to the published version of the manuscript.

Conflicts of interests

The authors declare no conflict of interest.

Abbreviation

Abbreviation	Full Name
AI	Artificial Intelligence
ANN	Artificial Neural Network
BC/IC	Boundary/Initial Conditions
CFD	Computational Fluid Dynamics
CNN	Convolutional Neural Network
DeepONet	Deep Operator Network
DTs	Digital Twins
EIS	Electrochemical Impedance Spectroscopy
FEA	Finite Element Analysis
FNO	Fourier Neural Operator
GAN	Generative Adversarial Network
LSCF	Lanthanum Strontium Cobalt Ferrite
MPC	Model Predictive Control
MSE	Mean Squared Error
OoD	Out-of-Distribution
PDE	Partial Differential Equation
PIAI	Physics-Informed Artificial Intelligence
PINN	Physics-Informed Neural Network
ROM	Reduced-Order Model
SOC	Solid Oxide Cell
SOEC	Solid Oxide Electrolysis Cell
SOFC	Solid Oxide Fuel Cell
TPB	Triple-Phase Boundary
UQ	Uncertainty Quantification
YSZ	Yttria-Stabilized Zirconia

Symbol

Symbol	Description	Unit
B	Boundary condition operator	-
E	Voltage/Potential	V
g	Boundary/Initial value function	-
J	Current density	A/cm^{-2}
L	Loss function	-
N	Differential operator	-
p	Partial pressure	atm or Pa
T	Temperature	°C
u_θ	Network output / Predicted field	-
α	Charge transfer coefficient	-
λ	Loss weighting factor	-

References

[1] Flis G, Wakim G. Solid oxide electrolysis: a technology status assessment. Technical report, CATF, 2023. Avalaible: https://cdn.catf.us/wp-content/uploads/2023/11/15092028/solid-oxide-electrolysis-report.pdf (accessed on 21 November 2025).

[2] Wu Z, Zhu P, Huang Y, Yao J, Yang F, *et al.* A comprehensive review of modeling of solid oxide fuel cells: from large systems to fine electrodes. *Chem. Rev.* 2025, 125(4):2184–2268.

[3] Yang Y, Lei J, Huang X, Liao Z, Liu Y, *et al.* Recent development in reversible solid oxide fuel cells: theory, integration and prospective. *ChemElectroChem* 2024, 11(6):e202300593.

[4] Taç V, Linka K, Sahli-Costabal F, Kuhl E, Tepole AB. Benchmarking physics-informed frameworks for data-driven hyperelasticity. *Comput. Mech.* 2024, 73(1):49–65.

[5] Zarabi Golkhatmi S, Asghar MI, Lund PD. A review on solid oxide fuel cell durability: latest progress, mechanisms, and study tools. *Renewable Sustainable Energy Rev.* 2022, 161:112339.

[6] Kang JL, Wang CC, Wong DSH, Jang SS, Wang CH. Digital twin model and dynamic operation for a plant-scale solid oxide fuel cell system. *J. Taiwan Inst. Chem. Eng.* 2021, 118:60–67.

[7] Testasecca T, Maniscalco MP, Brunaccini G, Airò Farulla G, Ciulla G, *et al.* Toward a digital twin of a solid oxide fuel cell microcogenerator: data-driven modelling. *Energies* 2024, 17(16):4140.

[8] Karniadakis GE, Kevrekidis IG, Lu L, Perdikaris P, Wang S, *et al.* Physics-informed machine learning. *Nat. Rev. Phys.* 2021, 3(6):422–440.

[9] Wu Y, Sicard B, Gadsden SA. Physics-informed machine learning: a comprehensive review on applications in anomaly detection and condition monitoring. *Expert Syst. Appl.* 2024, 255:124678.

[10] Raissi M, Perdikaris P, Karniadakis G. Physics-informed neural networks: a deep learning framework for solving forward and inverse problems involving nonlinear partial differential equations. *J. Comput. Phys.* 2019, 378:686–707.

[11] Ashraf H, Draz A. A comprehensive survey of artificial intelligence-based techniques for performance enhancement of solid oxide fuel cells: test cases with debates. *Artif. Intell. Rev.* 2024, 57(2):29.

[12] Sarwa B, Moz´dzierz M, Brus G. Artificial intelligence-based modeling of solid oxide fuel cells for improved transient prediction and control optimization. *J. Power Sources* 2025, 658:238281.

[13] Olowu TO, Westover TL, Casteel MJ. Physics-informed and machine learning-based design optimization of solid oxide fuel cells. *e-Prime Adv. Electr. Eng. Electron. Energy.* 2025, 13:101032.

[14] Zhang B, Harun NF, Zhou N, Oryshchyn D, Colon-Rodriguez JJ, *et al.* A real-time distributed solid oxide electrolysis cell (SOEC) model for cyber-physical simulation. *Appl. Energy.* 2025, 388:125607.

[15] Singh P, Sandhu A, Khan Y, Raman R, Barmavatu P, *et al.* Energy-efficient parameter estimation of solid oxide fuel cells under varying pressure conditions using the black widow optimization algorithm. *Front. Energy Res.* 2025, 13:1659232.

[16] Estrada NGA, Cervera RBM. Machine learning-based predictive modeling for solid oxide electrolysis cell (SOEC) electrochemical performance. *Appl. Sciences.* 2025, 15(17):9388.

[17] Lamagna M, Groppi D, Nastasi B. Reversible solid oxide cells applications to the building sector. *Int. J. Hydrogen Energy* 2023, 48(70):27033–27058.

[18] Tabish A, Patel H, Mani A, Schoonman J, Aravind P. Effect of H2S and HCl contaminants on nickel and ceria pattern anode solid oxide fuel cells. *Electrochim. Acta* 2022, 423:140592.

[19] Jang I, SA Carneiro J, Crawford JO, Cho YJ, Parvin S, *et al.* Electrocatalysis in solid oxide fuel cells and electrolyzers. *Chem. Rev.* 2024, 124(13):8233–8306.

[20] Liu H, Yu M, Tong X, Wang Q, Chen M. High temperature solid oxide electrolysis for green hydrogen production. *Chem. Rev.* 2024, 124(18):10509–10576.

[21] Li M, Wang J, Chen Z, Qian X, Sun C, *et al.* A comprehensive review of thermal management in solid oxide fuel cells: focus on burners, heat exchangers, and strategies. *Energies* 2024, 17(5):1005.

[22] Niakolas DK. Sulfur poisoning of Ni-based anodes for Solid Oxide Fuel Cells in H/C-based fuels. *Appl. Catal., A* 2014, 486:123–142.

[23] Zhou L, Mason JH, Li W, Liu X. Comprehensive review of chromium deposition and poisoning of solid oxide fuel cells (SOFCs) cathode materials. *Renewable Sustainable Energy Rev.* 2020, 134:110320.

[24] Cheng K, Xu H, Zhang L, Zhou J, Wang X, *et al.* Computational engineering of the oxygen electrode-electrolyte interface in solid oxide fuel cells. *npj Comput. Mater.* 2021, 7(1):119.

[25] Xu H, Cheng K, Chen M, Zhang L, Brodersen K, *et al.* Interdiffusion between gadolinia doped ceria and yttria stabilized zirconia in solid oxide fuel cells: experimental investigation and kinetic modeling. *J. Power Sources* 2019, 441:227152.

[26] Bernadet L, Buzi F, Baiutti F, Segura-Ruiz J, Dolado J, *et al.* Thickness effect of thin-film barrier layers for enhanced long-term operation of solid oxide fuel cells. *APL Energy.* 2023, 1(3):036101.

[27] Szymczewska D, Karczewski J, Chrzan A, Jasinski P. CGO as a barrier layer between LSCF electrodes and YSZ electrolyte fabricated by spray pyrolysis for solid oxide fuel cells. *Solid State Ionics* 2017, 302:113–117.

[28] Yue W, Li Y, Zheng Y, Wu T, Zhao C, *et al.* Enhancing coking resistance of Ni/YSZ electrodes: *in situ* characterization, mechanism research, and surface engineering. *Nano Energy* 2019, 62:64–78.

[29] Zhang W, Wei J, Yin F, Sun C. Recent advances in carbon-resistant anodes for solid oxide fuel cells. *Mater. Chem. Front.* 2023, 7(10):1943–1991.

[30] Riegraf M, Yurkiv V, Costa R, Schiller G, Friedrich KA. Evaluation of the effect of sulfur on the performance of nickel/gadolinium-doped ceria based solid oxide fuel cell anodes. *ChemSusChem.* 2017, 10(3):587–599.

[31] Vafaeenezhad S, Hanifi AR, Laguna-Bercero MA, Etsell TH, Sarkar P. Microstructure and long-term stability of Ni–YSZ anode supported fuel cells: a review. *Mater. Futures.* 2022, 1(4):042101.

[32] Chen-Wiegart YcK, Kennouche D, Scott Cronin J, Barnett SA, Wang J. Effect of Ni content on the morphological evolution of Ni-YSZ solid oxide fuel cell electrodes. *Appl. Phys. Lett.* 2016, 108(8):083903.

[33] Kröll L, De Haart LGJ, Vinke I, Eichel RA. Degradation mechanisms in solid-oxide fuel and electrolyzer cells: analytical description of nickel agglomeration in a Ni/YSZ electrode. *Phys. Rev. Appl.* 2017, 7(4):044007.

[34] He H, Hill JM. Carbon deposition on Ni/YSZ composites exposed to humidified methane. *Appl. Catal. A: Gen.* 2007, 317(2):284–292.

[35] Mikkola J, Couturier K, Talic B, Frangini S, Giacometti N, *et al.* Protective coatings for ferritic stainless steel interconnect materials in high temperature solid oxide electrolyser atmospheres. *Energies* 2022, 15(3):1168.

[36] Harrison C, Slater P, Steinberger-Wilckens R. A review of solid oxide fuel cell cathode materials with respect to their resistance to the effects of chromium poisoning. *Solid State Ionics* 2020, 354:115410.

[37] Pagliari M, Montinaro D, Martelli E, Campanari S, Donazzi A. Durability and kinetic effects of CO2-rich oxidizing streams on LSCF-based solid oxide fuel cells. *J. Power Sources* 2024, 613:234895.

[38] Zhao H, Li W, Wang H, Zhou J, Sun X, *et al.* Surface modification of La0.6Sr0.4Co0.2Fe0.8O3 cathode by infiltrating a-site deficient non-strontium La0.94Ni0.6Fe0.4O3 perovskite for solid oxide fuel cells. *Appl. Surf. Sci.* 2022, 572:151382.

[39] He F, Zhu F, Xu K, Xu Y, Liu D, *et al.* A highly oxygen reduction reaction active and CO2 durable high-entropy cathode for solid oxide fuel cells. *Appl. Catal. B Environ. Energy.* 2024, 355:124175.

[40] Yang Z, Guo M, Wang N, Ma C, Wang J, *et al.* A short review of cathode poisoning and corrosion in solid oxide fuel cell. *Int. J. Hydrogen Energy.* 2017, 42(39):24948–24959.

[41] Jeanmonod G, Diethelm S, Van Herle J. Poisoning effects of chlorine on a solid oxide cell operated in co-electrolysis. *J. Power Sources* 2021, 506:230247.

[42] Zeng Z, Qian Y, Zhang Y, Hao C, Dan D, *et al.* A review of heat transfer and thermal management methods for temperature gradient reduction in solid oxide fuel cell (SOFC) stacks. *Appl. Energy.* 2020, 280:115899.

[43] Zhang X, Wu M, Xiao L, Wang H, Liu Y, *et al.* Thermal stress in full-size solid oxide fuel cell stacks by multi-physics modeling. *Energies* 2024, 17(9):2025.

[44] Xu N, Zhang S, Zhou Q, Wang H, Zhao L, *et al.* Mechanistic study on the corrosion of (La,Sr)(Co,Fe)O3-δ cathodes induced by CO2. *Molecules* 2023, 28(22):7490.

[45] Nemati A, Rizvandi OB, Nakashima RN, Beyrami J, Frandsen HL. Multiscale multiphysics modeling of ammonia-fueled solid oxide fuel cell: effects of temperature and pre-cracking on reliability and performance of stack and system. *Appl. Energy.* 2024, 373:123913.

[46] Zhang B, Harun NF, Zhou N, Colon-Rodriguez JJ, Oryshchyn D, *et al.* A real-time multiphysics model of a pressurized solid oxide electrolysis cell (SOEC) for cyber-physical simulation. *Energy Convers. Manage.* 2023, 298:117778.

[47] Vijay P, Tadé MO. An adaptive non-linear observer for the estimation of temperature distribution in the planar solid oxide fuel cell. *J. Process Control.* 2013, 23(3):429–443.

[48] Wu X, Yang D, Wang J, Li X. Temperature gradient control of a solid oxide fuel cell stack. *J. Power Sources* 2019, 414:345–353.

[49] Wu X, Jiang J, Zhao W, Li X, Li J. Two-dimensional temperature distribution estimation for a cross-flow planar solid oxide fuel cell stack. *Int. J. Hydrogen Energy.* 2020, 45(3):2257–2278.

[50] Rauh A, Frenkel W, Kersten J. Kalman. Filter-based online identification of the electric power characteristic of solid oxide fuel cells aiming at maximum power point tracking. *Algorithms* 2020, 13(3):58.

[51] Sheng C, Zheng Y, Tian R, Xiang Q, Deng Z, *et al.* A comparative study of the kalman filter and the LSTM network for the remaining useful life prediction of SOFC. *Energies* 2023, 16(9):3628.

[52] Boushehri C, Cadigan C, Chmura C, Floerchinger G, Sullivan NP, *et al.* Experimental validation of model predictive control for solid oxide fuel cells. *J. Power Sources* 2023, 579:233271.

[53] De Avila Ferreira T, Wuillemin Z, Marchetti A, Salzmann C, Van Herle J, *et al.* Real-time optimization of an experimental solid-oxide fuel-cell system. *J. Power Sources* 2019, 429:168–179.

[54] Hassija V, Chamola V, Mahapatra A, Singal A, Goel D, *et al.* Interpreting black-box models: a review on explainable artificial intelligence. *Cognit. Comput.* 2024, 16(1):45–74.

[55] Rudin C. Stop explaining black box machine learning models for high stakes decisions and use interpretable models instead. *Nat. Mach. Intell.* 2019, 1(5):206–215.

[56] Latrach A, Malki ML, Morales M, Mehana M, Rabiei M. A critical review of physics-informed machine learning applications in subsurface energy systems. *Geoenergy Sci. Eng.* 2024, 239:212938.

[57] Meng C, Griesemer S, Cao D, Seo S, Liu Y. When physics meets machine learning: a survey of physics-informed machine learning. *Mach. Learn. Comput. Sci. Eng.* 2025, 1(1):20.

[58] Ma Z, Jiang G, Hu Y, Chen J. A review of physics-informed machine learning for building energy modeling. *Appl. Energy.* 2025, 381:125169.

[59] Langner E, Dehghani H, Hachemi ME, Belouettar–Mathis E, Makradi A, *et al.* Physics-based and data-driven modelling and simulation of solid oxide fuel cells. *Int. J. Hydrogen Energy.* 2024, 96:962–983.

[60] Huo H, Xu K, Cui L, Zhang H, Xu J, *et al.* Temperature gradient control of the solid oxide fuel cell under variable load. *ACS Omega* 2021, 6(42):27610–27619.

[61] Kobayashi K, Alam SB. Deep neural operator driven real time inference for nuclear systems to enable digital twin solutions. *Sci. Rep.* 2024, 14(1):2101.

[62] Laubscher R. Simulation of multi-species flow and heat transfer using physics-informed neural networks. *Phys. Fluids.* 2021, 33(8):087101.

[63] Le GT, Mastropasqua L, Adler SB, Brouwer J. Operando diagnostics of solid oxide fuel cell stack via electrochemical impedance spectroscopy simulation-informed machine learning. *ECS Trans.* 2021, 103(1):1201–1211.

[64] Chen H, Kätelhön E, Compton RG. Predicting voltammetry using physics-informed neural networks. *J. Phys. Chem. Lett.* 2022, 13(2):536–543.

[65] Niu Z, Zhao W, Wu B, Wang H, Lin WF, *et al.* π Learning: a performance-informed frame- work for microstructural electrode design. *Adv. Energy Mater.* 2023, 13(17):2300244.

[66] Tao J, Sciazko A, Onishi J, Ouyang Z, Komatsu Y, *et al.* Prediction of dynamic ni morphology changes in patterned Ni-YSZ anode with physics-informed neural networks. *J. Electrochem. Soc.* 2024, 171(5):054513.

[67] Li H, Wang Y, Zhu J, Han M. Performance map and operating condition optimization of industrial-size SOFCs using a PINN surrogate model. *Int. J. Hydrogen Energy* 2024, 50:1294–1307.

[68] Sciazko A, Komatsu Y, Shimura T, Shikazono N. Prediction of electrode microstructure evo- lutions with physically constrained unsupervised image-to-image translation networks. *npj Comput. Mater.* 2024, 10(1):49.

[69] Delpisheh M, Ebrahimpour B, Fattahi A, Siavashi M, Mir H, *et al.* Leveraging machine learning in porous media. *J. Mater. Chem. A* 2024, 12(32):20717–20782.

[70] Yang J, Zhang Y, Yang K, Sun K, Wei Y, *et al.* Optimization of operating conditions for industrial-size solid oxide electrolysis cells. *Int. J. Hydrogen Energy* 2025, 178:151525.

[71] Berardi M, Difonzo FV, Icardi M. Inverse physics-informed neural networks for transport models in porous materials. *Comput. Methods Appl. Mech. Eng.* 2025, 435:117628.

[72] Jang S, Kang Y, Bae KT, Park SH, Park YJ, *et al.* Digital twin of solid oxide electrochemical cells: from 3D microstructure reconstruction to multiphysics modeling. *Adv. Energy Mater.* 2025, 15(47):e03842.

[73] Gnatowski M, Buchaniec S, Brus G. The prediction of the polarization curves of a solid oxide fuel cell anode with an artificial neural network supported numerical simulation. *Int. J. Hydrogen Energy* 2023, 48(31):11823–11830.

[74] Bao J, Wang C, Xu Z, Koeppel B. Physics-informed machine learning with application to solid oxide fuel cell system modeling and optimization. Techical Report, PNNL–29124, 1569289, PNNL, 2019. Avalaible: https://www.osti.gov/biblio/1569289 (accessed on 21 November 2025).

[75] Buchaniec S, Gnatowski M, Brus G. Integration of classical mathematical modeling with an artificial neural network for the problems with limited dataset. *Energies* 2021, 14(16):5127.

[76] Buchaniec S, Gnatowski M, Hasegawa H, Brus G. A surrogate model of the butler-volmer equation for the prediction of thermodynamic losses of solid oxide fuel cell electrode. *Energies* 2023, 16(15):5651.

[77] Campbell F. Data-driven modeling of oxygen kinetics in La0.6Sr0.4Co0.2Fe0.8O3-δ (LSCF) for high-temperature reduction of CO2 in an electrolysis cell. Master's Thesis, West Virginia University Libraries, 2024.

[78] Wang D, Bao J, Xu Z, Koeppel B, Marina OA, *et al.* Machine learning tools set for natural gas fuel cell system design. *ECS Trans.* 2021, 103(1):2283–2292.

[79] Sarwa B, Moz´dzierz M, Brus G. Artificial intelligence-based modeling of solid oxide fuel cells for improved transient prediction and control optimization. *J. Power Sources* 2025, 658:238281.

[80] Ba L, Xiong X, Yang Z, Lei Z, Ge B, *et al.* A novel multi-physics and multi-dimensional model for solid oxide fuel cell stacks based on alternative mapping of BP neural networks. *J. Power Sources* 2021, 500:229784.

[81] Prokop TA, Buchaniec S, Szmyd J, Brus G. A parametric analysis of the long term performance of a solid oxide fuel cell anode. *Int. J. Heat Fluid Flow* 2024, 110:109583.

[82] Wu W, Wang C, Bian W, Hua B, Gomez JY, *et al.* Root cause analysis of degradation in protonic ceramic electrochemical cell with interfacial electrical sensors using data-driven machine learning. *Adv. Sci.* 2023, 10(30):2304074.

[83] Christopher GG, Olalekan OR, Huguette Maeva MN, Hassan B, Sayed HA. AI-augmented digital twin framework for predictive thermo-mechanical degradation monitoring in solid oxide fuel cell stacks: integration of multi-physics models and uncertainty quantification. *Ceram. Int.* 2025.

[84] Patel R, Bhartiya S, Gudi RD. Neural network-based model predictive control framework incorporating first-principles knowledge for process systems. *Ind. Eng. Chem. Res.* 2025, 64(18):9287–9302.

[85] Rauh A, Senkel L, Kersten J, Aschemann H. Reliable control of high-temperature fuel cell systems using interval-based sliding mode techniques. *IMA J. Math. Control Inf.* 2016, 33(2):457–484.

[86] Huang B, Qi Y, Murshed AKMM. *Dynamic Modelling and Predictive Control in Solid Oxide Fuel Cells: First Principle and Data-Based Approaches*, 1st ed. Hoboken: John Wiley & Sons, 2013.

[87] Huang B, Qi Y, Murshed M. Solid oxide fuel cell: perspective of dynamic modeling and control. *IFAC Proc.* 2010, 43(5):133–146.

[88] Bove R, Ubertini S, Bansal NP. *Modeling Solid Oxide Fuel Cells*, 1st ed. Dordrecht: Springer, 2008.

[89] Jagtap AD, Kharazmi E, Karniadakis GE. Conservative physics-informed neural net-works on discrete domains for conservation laws: applications to forward and inverse problems. *Comput. Methods Appl. Mech. Eng.* 2020, 365:113028.

[90] Rauh A, Kersten J, Frenkel W, Kruse N, Schmidt T. Physically motivated structuring and optimization of neural networks for multi-physics modelling of solid oxide fuel cells. *Math. Comput. Modell. Dyn. Syst.* 2021, 27(1):586–614.

[91] Forgione M, Piga D. *dynoNet*: a neural network architecture for learning dynamical systems. *Int. J. Adapt. Control Signal Process.* 2021, 35(4):612–626.

[92] Wang S, Yu X, Perdikaris P. When and why pinns fail to train: a neural tangent kernel perspective. *J. Comput. Phys.* 2022, 449:110768.

[93] Tancik M, Srinivasan PP, Mildenhall B, Fridovich-Keil S, Raghavan N, *et al.* Fourier features let networks learn high frequency functions in low dimensional domains. *Adv. Neural Inf. Process. Syst.* 2020, 33:7537–7547.

[94] Sitzmann V, Martel JNP, Bergman AW, Lindell DB, Wetzstein G. Implicit neural representations with periodic activation functions. *Adv. Neural Inf. Process. Syst.* 2020, 33:7462–7473.

[95] Jagtap AD, Karniadakis GE. Extended physics-informed neural networks (XPINNs): a generalized space-time domain decomposition based deep learning framework for nonlinear partial differential equations. *Commun. Comput. Phys.* 2020, 28(5):2002–2041.

[96] Hu Z, Jagtap AD, Karniadakis GE, Kawaguchi K. When do extended physics-informed neural networks (XPINNs) improve generalization? *SIAM J. Sci. Comput.* 2022, 44(5):A3158–A3182.

[97] Shukla K, Jagtap AD, Karniadakis GE. Parallel physics-informed neural networks via domain decomposition. *J. Comput. Phys.* 2021, 447:110683.

[98] Penwarden M, Zhe S, Narayan A, Kirby RM. Multifidelity modeling for physics-informed neural networks (PINNs). *J. Comput. Phys.* 2022, 451:110844.

[99] Meng X, Babaee H, Karniadakis GE. Multi-fidelity bayesian neural networks: algorithms and applications. *J. Comput. Phys.* 2021, 438:110361.

[100] Chi Y, Yokoo K, Nakajima H, Ito K, Lin J, *et al.* Optimizing the homogeneity and efficiency of a solid oxide electrolysis cell based on multiphysics simulation and data-driven surrogate model. *J. Power Sources* 2023, 562:232760.

[101] Yang L, Meng X, Karniadakis GE. B-PINNs: bayesian physics-informed neural networks for forward and inverse PDE problems with noisy data. *J. Comput. Phys.* 2021, 425:109913.

[102] Zhou X, Chen B, Gui Y, Cheng L. Conformal prediction: a data perspective. *ACM Comput. Surv.* 2025, 58(2).

[103] Chee KY, Hsieh MA, Pappas GJ. Uncertainty quantification for learning-based MPC using weighted conformal prediction. In *Proceedings of the 2023 62nd IEEE Conference on Decision and Control*, Singapore, December 13–15, 2023, pp. 342–349.

[104] Žnidaricˇ L, Nusev G, Morel B, Mougin J, Juricˇic´ Đ, *et al.* Evaluating uncertainties in electrochemical impedance spectra of solid oxide fuel Cells. *Appl. Energy* 2021, 298:117101.

[105] Boonma K, Mesgarpour M, NajmAbad JM, Alizadeh R, Mahian O, *et al.* Prediction of battery thermal behaviour in the presence of a constructal theory-based heat pipe (CBHP): a multiphysics model and pattern-based machine learning approach. *J. Energy Storage* 2022, 48:103963.

[106] Cho G, Zhu D, Campbell JJ, Wang M. An LSTM-PINN hybrid method to estimate lithium-ion battery pack temperature. *IEEE Access* 2022, 10:100594–100604.

[107] Kang S, Park G, Kum D. A transfer learning physics-informed neural network framework for solving multi-coupled partial differential equations with complex geometries: fuel cell case study. SSRN 2025.

[108] Wang J, Peng Q, Meng J, Liu T, Peng J, *et al.* A physics-informed neural network approach to parameter estimation of lithium-ion battery electrochemical model. *J. Power Sources* 2024, 621:235271.

[109] Salem NM, Shaheen MAM, Hasanien HM. Novel reinforcement learning technique based parameter estimation for proton exchange membrane fuel cell model. *Sci. Rep.* 2024, 14(1):27475.

[110] Ko T, Kim D, Park J, Lee SH. Physics-informed neural network for long-term prognostics of proton exchange membrane fuel cells. *Appl. Energy.* 2025, 382:125318.

[111] Polo-Molina A, Portela J, Rozas LAH, González RC. Modeling membrane degradation in pemelectrolyzers with physics-informed neural networks, 2025.

[112] Chen BR, Kunz MR, Tanim TR, Dufek EJ. A machine learning framework for early detection of lithium plating combining multiple physics-based electrochemical signatures. *Cell Rep. Phys. Sci.* 2021, 2(3):100352.

[113] Firoozi R, Sattarzadeh S, Dey S. Cylindrical battery fault detection under extreme fast charging: a physics-based learning approach. *IEEE Trans. Energy Convers.* 2022, 37(2):1241–1250.

[114] Pozzi A, Moura S, Toti D. A neural network-based approximation of model predictive control for a lithium-ion battery with electro-thermal dynamics. In *Proceedings of the 2022 IEEE 17th International Conference on Control & Automation*, Naples, Italy, June 27–30, 2022, pp. 160–165.

[115] Madani SS, Shabeer Y, Fowler M, Panchal S, Chaoui H, *et al.* Artificial intelligence and digital twin technologies for intelligent lithium-ion battery management systems: a comprehensive review of state estimation, lifecycle optimization, and cloud-edge integration. *Batteries* 2025, 11(8):298.

[116] Marcato A, Santos JE, Liu C, Boccardo G, Marchisio D, *et al.* Modeling the 4D discharge of lithium-ion batteries with a multiscale time-dependent deep learning framework. *Energy Storage Mater.* 2023, 63:102927.

[117] Zhang M, Amiri A, Xu Y, Bastin L, Clark T. Self-adaptive digital twin of fuel cell for remaining useful lifetime prediction. *Int. J. Hydrogen Energy.* 2024, 89:634–647.